

1                                   **Surface water and groundwater: Unifying**  
2                                   **conceptualization and quantification of the two “water**  
3                                   **worlds”**

4  
5  
6 Brian Berkowitz<sup>1</sup>, Erwin Zehe<sup>2</sup>

7  
8 1. Department of Earth and Planetary Sciences, Weizmann Institute of Science, Rehovot  
9     7610001, Israel

10 2. Karlsruhe Institute of Technology (KIT), Karlsruhe, Germany

11  
12 *Correspondence to:* Brian Berkowitz (brian.berkowitz@weizmann.ac.il)

13  
14  
15 **Abstract.**

16  
17 While both surface water and groundwater hydrological systems exhibit structural, hydraulic  
18 and chemical heterogeneity, and signatures of self-organisation, modelling approaches  
19 between these two “water world” communities generally remain separate and distinct. To  
20 begin to unify these water worlds, we recognize that preferential flows, in a general sense, are  
21 a manifestation of self-organisation; they hinder perfect mixing within a system, due to a  
22 more “energy efficient” and hence faster throughput of water and matter. We develop this  
23 general notion by detailing the role of preferential flow for residence times and chemical  
24 transport, as well as for energy conversions and energy dissipation associated with flows of  
25 water and mass. Our principal focus is on the role of heterogeneity and preferential flow and  
26 transport of water and chemical species. We propose, essentially, that related  
27 conceptualizations and quantitative characterisations can be unified in terms of a theory that  
28 connects these two water worlds in a dynamic framework. We discuss key features of fluid  
29 flow and chemical transport dynamics in these two systems – surface water and groundwater  
30 – and then focus on chemical transport, merging treatment of many of these dynamics in a  
31 proposed quantitative framework. We then discuss aspects of a unified treatment of surface  
32 water and groundwater systems in terms of energy and mass flows, and close with a reflection  
33 on complementary manifestations of self-organisation in spatial patterns and temporal  
34 dynamic behaviour.

35  
36  
37  
38 **Keywords:** Chemical transport, Continuous Time Random Walk (CTRW), self-organisation,  
39 preferential flow

## 44 1 INTRODUCTION

45 While surface and subsurface flow and transport of water and chemicals are strongly  
46 interrelated, the catchment hydrology (“surface water”) and groundwater communities are  
47 split into two “water worlds”. The communities even separate terminology, writing “surface  
48 water” as two words but “groundwater” as one word!

49 At a very general level, it is well recognized that both catchment systems and groundwater  
50 systems exhibit enormous structural and functional heterogeneity, which are, e.g., manifested  
51 through the emergence of preferential flow and space-time distributions of water, chemicals,  
52 sediments and colloids, and energy across all scales and within/across compartments (soil,  
53 aquifers, surface rills and river networks, full catchment systems, and vegetation). Dooge  
54 (1986) was among the first hydrologists who distinguished between different types of  
55 heterogeneity – namely, between stochastic and organised/structured variability – and  
56 reflected upon how these forms affect predictability of hydrological dynamics. He concluded  
57 that most hydrological systems fall into Weinberg’s (1975) category of organised complexity  
58 – meaning that they are too heterogeneous to allow pure deterministic handling but exhibit too  
59 much organisation to enable pure statistical treatment.

60 A common way to define spatial organisation of a physical system is through its distance  
61 from the maximum entropy state (Kondepudi and Prigogine, 1998; Kleidon, 2012). Isolated  
62 systems, which do not exchange energy, mass, or entropy with their environment, evolve due  
63 to the second law of thermodynamics to a perfectly mixed “dead state” called thermodynamic  
64 equilibrium. In such cases, entropy is maximized and Gibbs free energy is minimized,  
65 because all gradients have been dissipated by irreversible processes. Hydrological systems  
66 are, however, open systems, as they exchange mass (water, chemicals, sediments, colloids),  
67 energy and entropy across their system boundaries with their environment. Hydrological  
68 systems may hence persist in a state far from thermodynamic equilibrium. They may even  
69 evolve to states of a lower entropy, and thus stronger spatial organisation, for instance through  
70 steepening of gradients, for example, in topography, or in the emergence of structured  
71 variability of system characteristics or network-like structures. Such a development is referred  
72 to as “self-organisation” (Haken, 1983) because local scale dissipative interactions, which are  
73 irreversible and produce entropy, lead to ordered states or dynamic behaviours at the (macro-)  
74 scale of the entire system. Self-organisation requires free energy transfer into the system to  
75 perform the necessary physical work, self-reinforcement through a positive feedback to assure  
76 “growth” of the organised structure/patterns in space, and the export of the entropy which is  
77 produced within the local interactions to the environment (Kleidon, 2012).

78 Manifestations of self-organisation in *catchment systems* are manifold. The most obvious  
79 one is the persistence of smooth topographic gradients (Reinhardt and Ellis, 2015; Kleidon et  
80 al. 2012), which reflect the interplay of tectonic uplift and the amount of work water and biota  
81 have performed to weather and erode solid materials, to form soils and create flow paths.  
82 Although these processes are dissipative and produce entropy, they nevertheless leave  
83 signatures of self-organisation in catchment systems. These are expressed, for instance,  
84 through the soil catena – a largely deterministic arrangement of soil types along the  
85 topographic gradient of hillslopes (Milne, 1931; Zehe et al., 2014) – and even more strongly  
86 through the formation of rill and river networks (Fig. 1) at the hillslope and catchment scales

87 (Howard, 1990; Paik and Kumar, 2010; Kleidon et al., 2013). These networks form because  
88 flow in rills is, in comparison to sheet flow, associated with a larger hydraulic radius, which  
89 implies less frictional energy dissipation per unit volume of flow. This causes higher flow  
90 rates, which in turn may erode more sediment. As a result, these networks commonly increase  
91 the efficiency in transporting water, chemicals, sediments and energy through hydrological  
92 systems, which results also in increased kinetic energy transport through the network and  
93 across system boundaries.

94 In contrast, the term self-organisation is rarely applied to *groundwater systems*, except in  
95 the context of positive/negative feedbacks during processes of precipitation and dissolution  
96 (e.g., Worthington and Ford, 2009). We argue, though, that the subsurface, too, displays some  
97 characteristics of (partial) self-organisation. This is manifested, in particular, through  
98 ubiquitous, spatially correlated, anisotropic patterns of aquifer structural and hydraulic  
99 properties, particularly in non-Gaussian systems (Bardossy, 2006), as these have much  
100 smaller entropy compared to spatially uncorrelated patterns. The emergence and persistence  
101 of preferential pathways even in homogeneous sand packs (e.g., Hoffman et al., 1996; Oswald  
102 et al., 1997; Levy and Berkowitz, 2003) is a striking example of formation of a self-organised  
103 pattern of “smooth fluid pressure gradients”.

104



105

106 **Figure 1** Hillslope scale rill networks developed during an overland flow event at the  
107 Dornbirner Ach Austria (left panel, we gratefully acknowledge the Copyright holder © Ulrike  
108 Scherer KIT) and the South Fork of Walker Creek in California (right panel, we gratefully  
109 acknowledge the Copyright holder © James Kirchner ETH Zürich)

110

111 Our general recognition is that hydrological systems exhibit – below and above ground –  
112 both (structural, hydraulic and chemical) heterogeneity and signatures of (self-)organisation.  
113 We propose that all kinds of preferential flow paths/flow networks veining the land surface  
114 and the subsurface are prime examples of spatial organisation (Bejan et al., 2008; Rodriguez-  
115 Iturbe and Rinaldo, 2001) because they exhibit, independently of their genesis, similar  
116 topological characteristics. Our starting point to unify both water worlds is the recognition  
117 that any form of preferential flow is a manifestation of self-organisation, because it hinders  
118 perfect mixing within a system and implies a more “energy efficient” and hence faster  
119 throughput of water and matter (Rodriguez-Iturbe et al., 1999; Zehe et al., 2010; Kleidon et  
120 al., 2013). This general notion can be elaborated further by detailing the role of preferential  
121 flow for transport of mass and chemical species, and related fingerprints in travel distances or

122 travel times, as well as for energy conversion and energy dissipation associated with flows of  
123 water.

124 In terms models, hydrological modelling (and hydrological theory) attempts to predict  
125 how processes described by equations evolve in and interact with a structured heterogeneous  
126 domain (i.e., hydrological landscape). However, our key argument that both systems are  
127 subject to similar manifestations of self-organisation does not imply proposed use of a single  
128 model. Rather, we argue that similar conceptualisations and methods of quantification –  
129 whether related to preferential flow paths, dynamics and patterning of chemical transport and  
130 reactivity, or characterization in terms of energy dissipation and entropy production, for  
131 example – can and should be applied to both catchment and groundwater systems, to the  
132 benefit of both research communities. The main focus of this contribution is on the role of  
133 heterogeneity and preferential flow and transport of water and chemical species. At a general  
134 level, we show that preferential flow causes deviations from the maximum entropy state,  
135 though these deviations have different manifestations depending on whether we observe  
136 solute transport in space or in time. Based on this insight, we propose, essentially, that related  
137 conceptualisations and quantitative characterisations can be unified in terms of a theory that is  
138 applicable in catchment and groundwater systems, and thus connects these two “water  
139 worlds”.

140 We first discuss key features of fluid flow and chemical transport dynamics in these two  
141 systems – catchments (including surface water) and groundwater – using the (often distinct)  
142 terminology of each of these “water world” research communities. We outline the particular  
143 questions, methods, limitations, and uncertainties in each “world” (Section 2). We then focus  
144 on chemical transport, merging treatment of many of these dynamics in a proposed  
145 quantitative framework, and providing specific examples (Section 3). More specifically,  
146 Section 3 first defines specific conceptual and quantitative tools, and within this context,  
147 introduces a continuous time random walk (CTRW) modelling framework with a clear  
148 connection to microscale physics and to the well-known advection-dispersion equation.  
149 Section 3 then offers new insights, in terms of contrasting power law and inverse gamma  
150 distributions – used in the groundwater literature to describe different travel time distributions  
151 that control long tailing in breakthrough curves – to gamma distributions used more often in  
152 the surface water (catchment system) literature. This analysis is a basis for suggesting how  
153 surface water systems (catchment response to chemical transport) can be treated within the  
154 CTRW framework. Final conclusions and perspectives appear in Section 4. Throughout, we  
155 attempt to offer an innovative synthesis of concepts and methods from the generally disparate  
156 surface water (catchment hydrology) and groundwater research communities. Each  
157 community has developed sophisticated modelling and measurement capabilities – which  
158 have led to significant scientific advances over the last two decades – that could benefit the  
159 other community and help address outstanding, unsolved problems.

160 Before proceeding, we emphasise that our use of the term “two water worlds” throughout  
161 this paper is intended to highlight the disparate catchment and groundwater communities, and  
162 is not used in the specific context of mobile-immobile water in the root zone (McDonnell,  
163 2014), as discussed at the end of Section 3.1.

## 164 2 TWO WATER WORLDS – UNIQUE, DIFFERENT AND SIMILAR

### 165 2.1 Governing laws of fluid flow, the momentum balance and energy 166 dissipation

167 In both water worlds, a major focus is on travel distances, as well as travel times  
168 (residence times) of water, as they provide the main link between water quantity and quality  
169 (Hrachowitz et al., 2016). Catchment hydrology deals also with extremes, i.e., floods and  
170 droughts, as well as land surface-atmosphere feedbacks, fluvial geomorphology and eco-  
171 hydrology.

172 From the outset, we recognise that predictions of water dynamics in catchment and aquifer  
173 systems require joint treatment of their mass, momentum and energy balances. Catchment  
174 science and modelling has, traditionally, a strong focus on catchment mass and (in part)  
175 energy balances, as evaporation and transpiration release energy in the form of latent heat to  
176 the atmosphere. The momentum balance is treated in an implicit conceptualised manner, as  
177 detailed below. Predictions of fluid flow in groundwater systems rely on the joint treatment of  
178 the mass and the stationary momentum balances using Darcy’s law, while the energy balance  
179 appears at first sight of low importance.

180 Chemical transport and travel times through hydrological systems are, however, strongly  
181 related to both the momentum and the energy balances, because they jointly control the  
182 spectrum of fluid velocities and the direction of streamlines. The governing equations that  
183 characterise water flow velocities along the land surface and in groundwater systems are  
184 simplifications of the Navier-Stokes equations (Eq. 1), which describe the momentum balance  
185 of the fluid as an interplay of driving forces and hindering frictional forces:

$$186 \quad \rho \frac{\partial \mathbf{v}}{\partial t} + (\mathbf{v} \cdot \nabla) \mathbf{v} = -\nabla p - \rho \mathbf{g} + \eta \Delta^2 \mathbf{v} \quad (\text{Eq. 1})$$

187 where  $\mathbf{v}$  (m s<sup>-1</sup>) is the fluid velocity vector,  $\mathbf{g}$  (m s<sup>-2</sup>) the gravitation acceleration vector,  $\rho$  (kg  
188 m<sup>-3</sup>) the water density, and  $\eta$  the dynamic viscosity (kg m<sup>-1</sup> s<sup>-1</sup>) of the fluid.

#### 189 2.1.1 Surface water flow and Manning’s law

190 Overland and channel flow are driven by surface topography, or more precisely, by  
191 gravitational potential energy differences, but only minute amounts of these energy  
192 differences are converted into kinetic energy of the flow (Loritz et al., 2019), while the rest is  
193 dissipated. Surface water flow velocity is often characterised by Manning’s law (Eq. 2), a  
194 steady-state, one-dimensional approximation of the Navier-Stokes equation that neglects  
195 inertial acceleration for the case of turbulent shear stress and thus turbulent energy  
196 dissipation. Fluid velocity grows proportional to the square root of the driving hydraulic head  
197 gradient; the latter corresponds to the potential energy of a unit mass of water:

$$198 \quad \mathbf{v}_{\text{surface}} = -\frac{R^{\frac{2}{3}}}{n} \sqrt{2g \nabla_{x,y}(h+z)} = -\frac{R^{\frac{2}{3}}}{n} \sqrt{2g \nabla_{x,y} \Phi_H} \quad (\text{Eq. 2})$$

199 where  $\mathbf{v}_{\text{surface}}$  (m s<sup>-1</sup>) is the overland flow velocity vector,  $R$  (m) the hydraulic radius defined  
200 as the ratio of the wetted cross-section  $A_{\text{wet}}$  (m<sup>2</sup>) to the wetted perimeter  $U_{\text{wet}}$  (m),  $n$  is  
201 Manning’s roughness (m<sup>-1/3</sup>),  $z$  (m) is topographical elevation,  $h$  (m) is depth of the flow, and  
202  $\Phi$  (m) is the total hydraulic head.

203 Moreover, as friction occurs mainly at the contact line between the fluid and the solid, the  
204 hydraulic radius  $R$  (m) can be used to scale the ratio between driving gravity force and the

205 hindering frictional dissipative force. Kleidon et al. (2013) classified this as a “weak form” of  
 206 dissipative interaction between fluid and solid. In this context, they showed that overland flow  
 207 in rills implies, due to the larger hydraulic radius, a smaller dissipative loss per unit volume  
 208 and thus a higher energy efficiency compared to sheet flow. Along the same line, they showed  
 209 that flow in a smaller number of wider channels is more efficient than flow in a higher  
 210 number of narrower channels. Both effects, flow in rills and channelling, lead to a higher fluid  
 211 velocity, and thus a higher power (kinetic energy) flux through the network. Note that a 10%  
 212 faster fluid velocity implies 30% more power as the latter grows with the cube of the fluid  
 213 velocity.

## 214 **2.1.2 Subsurface flow and Darcy’s law**

215 Flow through subsurface porous media, on the other hand, is driven by the gradient in  
 216 total hydraulic head, reflecting differences in gravitational potential, matric potential and  
 217 pressure potential energies as described in the respective forms of Darcy’s law (Eq. 3). The  
 218 latter is also a steady state, one dimensional approximation of the Navier-Stokes equation  
 219 neglecting the inertial terms. However, in this case flow is essentially laminar and dissipative  
 220 frictional losses in the porous medium are so much larger than in open surface flow, that  
 221 kinetic energy can be neglected. When solving the Darcy law (Eq. 3, first line) for the  
 222 interstitial travel velocities and defining the flow resistance as inverse hydraulic conductivity,  
 223 one obtains a form of the Darcy law (Eq. 3, second line) which is similar to Manning’s law  
 224 (Eq. 2). The main difference arises from the different dependencies on the hydraulic head  
 225 gradient, reflecting the turbulent and laminar flow regimes, respectively:

$$\begin{aligned}
 227 \quad \mathbf{q}_{vadose} &= -k(\theta)\nabla(\psi + z), \quad \mathbf{q}_{gw} = -k_s\nabla(H + z) \\
 228 \quad \mathbf{v}_{vadose} &= -\frac{1}{\theta R(\theta)}\nabla\Phi_{vadose}, \quad \mathbf{v}_{gw} = -\frac{1}{\theta_s R_s}\nabla\Phi_{gw} \text{ (Eq. 3)} \\
 229 \quad R(\theta) &= 1/k(\theta), R = 1/k_s, \Phi_{vadose} = (\psi + z), \Phi_{gw} = (H + z)
 \end{aligned}$$

230  
 231 where  $\mathbf{q}_{vadose}$  and  $\mathbf{q}_{gw}$  ( $\text{m s}^{-1}$ ) are water flux vectors (filter velocities) in the partially saturated  
 232 and saturated zones, respectively,  $\mathbf{v}_{vadose}$  and  $\mathbf{v}_{gw}$  ( $\text{m s}^{-1}$ ) are the respective interstitial travel  
 233 velocities,  $\theta$  and  $\theta_s$  are the soil water content (-) and the porosity (-),  $k(\theta)$  and  $k_s$  ( $\text{m s}^{-1}$ ) are the  
 234 partially saturated and saturated hydraulic conductivity,  $\psi$  (m) and  $H$  (m) denote the capillary  
 235 pressure and pressure potentials, and  $\Phi_{vadose}$  and  $\Phi_{gw}$  are total hydraulic heads in the partially  
 236 saturated and saturated zones.

237 The strikingly high dissipative nature of porous media flow becomes obvious when  
 238 recalling that the driving matric potential gradients in the vadose zone are often orders of  
 239 magnitude larger than  $1 \text{ m m}^{-1}$ . This implies a capillary acceleration term much larger than  
 240 Earth’s gravitational acceleration  $g$  ( $\text{m s}^{-2}$ ), yet fluid velocities in the porous matrix are several  
 241 orders of magnitude smaller than in surface water systems. However, the generally much  
 242 slower fluid velocity in groundwater systems does not impose a slow hydraulic response time  
 243 during rainstorms; on the contrary, aquifers may release – almost instantaneously – “older”,  
 244 pre-event water into a catchment outlet stream. This apparent paradox – referred to often as  
 245 the “old-new water paradox” (Kirchner, 2003) – is explained by propagation of pressure  
 246 waves. Shear or compression waves (or waves in general) transport momentum and energy

247 through continua *without an associated transport of mass or particles* (Everett, 2013;  
248 Goldstein, 2013); and group velocity (or “celerity”) is many orders of magnitude larger than  
249 the fluid velocity in aquifer systems (McDonnell and Beven, 2014). Today, it is known that  
250 depending on landscape setting, antecedent wetness conditions, and the dominant runoff  
251 mechanisms, pre-event water fractions in storm runoff can vary from near zero to more than  
252 60% of storm water having an isotopic signature different from that of rainfall (Sklash and  
253 Farvolden, 1979; Sklash et al., 1996; Blume et al., 2008).

### 254 **2.1.3 Preferred flow paths as maximum power structures and non-Fickian** 255 **transport**

256 Flow velocity within subsurface preferential pathways (macropores, pipes, fractures) is  
257 known to be much faster than matrix flow (Beven and Germann, 1982, 2013). This is caused  
258 not only by the vanishing capillary forces, but also, largely, by the strong reduction in  
259 frictional dissipation in macropores compared to flow in the porous matrix. Viscous  
260 dissipation in preferential pathways occurs, similar to open channel flow, mainly at the  
261 contact line between fluid and solid, i.e., the wetted perimeter of the macropore, which  
262 implies – similar to the case of rill and river networks – a larger hydraulic radius and thus a  
263 much more energy efficient flow (Zehe et al., 2010). Darcy’s law is hence inappropriate to  
264 characterise preferential flow (Germann, 2018). Clearly, rapid localised flow and transport in  
265 preferential pathways hinders the transition from imperfectly mixed stochastic advective  
266 transport in the near field to well mixed advective dispersive transport in the far field.  
267 Predictions of solute plumes and travel times in the near field are thus challenging as this  
268 requires detailed knowledge of the velocity field, while transport at the well-mixed Fickian  
269 limit depends on the average fluid velocity and the dispersion coefficient (Simmons, 1982;  
270 Sposito et al., 1986; Bodin, 2015).

271 Although the revisited laws, interactions and phenomena are well known, we suggest that  
272 the energy point of view yields a unifying perspective to explain why macropore, rill and river  
273 networks are the preferred (preferential) pathways for water flow on land and below. One  
274 might hence expect that water flows along the path of maximum power (Howard, 1990;  
275 Kleidon, 2013), which is the product of the flow velocity times the driving potential  
276 difference. The paths of maximum power correspond in the case of constant friction to the  
277 path of steepest descent in hydraulic head, while in the case of a constant gradient, it  
278 corresponds to the path of minimum flow resistance (Zehe et al., 2010). From the discussion  
279 above, we further conclude that catchment hydrology and groundwater hydrology are  
280 inseparable. We can neither separate a river from its catchment and its subsurface, nor an  
281 aquifer from the land surface and the catchment. Both stream flow response to rainfall and  
282 groundwater are composed of “waters of different ages”, reflecting the ranges of overland  
283 flow, subsurface storm flow and base-flow contributions with their specific velocities, usually  
284 non-Fickian travel time distributions, and chemical signatures.

285 In the following, we elaborate briefly on the specific model paradigms in catchment and  
286 groundwater hydrology with an emphasis on preferential pathways for fluid flow and  
287 chemical transport, and on the resulting ubiquitous, anomalous early and late time arrivals of  
288 chemicals to measurement outlets.

## 289 **2.2 Catchment hydrology from the water balance to solute transport**

### 290 **2.2.1 The catchment concept and the duality in water balance modelling**

291 Catchment hydrology developed largely as an engineering discipline around traditional  
292 tasks of designing and operating reservoirs, flood risk assessment and water resources  
293 management (Sivapalan, 2018). Although the catchment concept is elementary to these tasks,  
294 we think it worthwhile to reflect briefly on it here. The watershed boundary delimits a control  
295 volume where the streamlines are expected to converge into the river network, hence ideally,  
296 the entire set of surface and subsurface runoff components feeds the stream. We can thus  
297 characterise the water balance of an ideally closed catchment control volume based on  
298 observations of rainfall input and stream flow response (with uncertainty). Even more  
299 importantly, the catchment water balance can be solved without an explicit treatment of the  
300 momentum balance, because flow lines end up in the stream.

301 This is a twofold blessing. First, hydrological models can be benchmarked against integral  
302 water balance observations. We posit that this unique property of catchments is *the* reason  
303 why integral conceptual hydrological models, which largely ignore the momentum balance,  
304 allow successful predictions of stream flow the catchment outlet (Sivapalan, 2018). As  
305 conceptual models directly address processes at the system level without accounting for  
306 subscale mechanistic reasons, their application is often referred to as “top down” modelling.  
307 The other end of the model spectrum consists of physics-based, spatially distributed models,  
308 originally proposed by the blueprint of Freeze and Harlan (1969), which follow a “bottom up”  
309 mechanistic paradigm. These models are thus also referred to as reductionist models. While  
310 the pros and cons of top down conceptual models and bottom up physics-based models have  
311 been discussed extensively, we agree with Hrachowitz and Clark (2017) that they offer  
312 complementary merits as detailed below. As an aside, it is interesting to reflect why  
313 conceptual models do not exist in the field of, e.g., meteorology. We suggest that this is  
314 because atmospheric flows are not governed by mechanisms similar to catchments, which  
315 implies that the amount of air mass flowing from one location to another cannot be predicted  
316 without knowing the flow lines.

### 317 **2.2.2 Top down modelling of the catchment water balance**

318 Top down conceptual hydrological models simulated water storage, redistribution and  
319 release within the catchment system through combination of non-linear and linear reservoirs,  
320 characterised by effective state variable and effective parameters and effective fluxes  
321 (Savenije and Hrachowitz, 2017). Due to their mathematical simplicity, conceptual models  
322 are straightforward to code. With the advent of combinatorial optimization methods for  
323 automated parameter search, and fast computers (Duan et al., 1992; Bardossy and Singh,  
324 2008; Vrugt and Ter Braak, 2011), these models became, at first sight, also straightforward to  
325 apply. Automated, random parameter search led, however, to the discovery of the well-known  
326 equifinality problem – namely, that several model structures or parameter sets may reproduce  
327 the target data in an acceptable manner (Beven and Binley, 1992), within the calibration and  
328 validation period, but these models and parameter sets yield uncertain future predictions (e.g.,  
329 Wagener et al., 2006). Equifinality and related parameter uncertainty arises from the ill-posed  
330 nature of inverse parameter estimation and from parameter interactions in the equations.  
331 While the first problem can be tackled using multi-objective and multiresponse calibration (e.g.,



332 Mertens et al., 2004; Ebel and Logue, 2006; Fencia et al., 2007), the latter is inherent to the  
333 model equations regardless of whether they are conceptual (as shown by Bardossy (2007) for  
334 the Nash cascade), or physically based (as shown by, e.g., Klaus and Zehe (2010) and Zehe et  
335 al. (2014)).

336 A well-known shortcoming of conceptual models is that their key parameters cannot be  
337 measured directly. This motivated numerous parameter regionalization efforts (He et al.,  
338 2011a) to relate conceptual parameters to measurable catchment characteristics, typically  
339 broadly available data on soils (including texture), land use, and topography. As a  
340 consequence, such functions have been derived successfully, for example, to relate parameters  
341 of the soil moisture accounting scheme to soil type and land use (as shown by, e.g., Hundecha  
342 and Bardossy, 2004; Samaniego and Bardossy, 2006; He et al., 2011b; Singh et al., 2016) or  
343 parameters of the soil moisture accounting of the mHm (Samaniego et al., 2010) to soil  
344 textural data. As such, relations are landscape-specific and they require a new calibration  
345 when moving to new target areas. This is of course possible if high quality discharge data are  
346 available. Yet, due to the incompatibility between the corresponding measurement and  
347 observations scales, these regionalisation functions are not straightforwardly explained using  
348 physical reasoning. This is true even if soil moisture accounting from soil physics is used,  
349 e.g., the Brooks and Corey (1964) soil water retention curve, as in the case of the mHm  
350 model.

351 Savenije (2010) and Fencia et al. (2011) significantly improved the link between  
352 conceptual models and landscape structure in their flexible model framework. The key idea is  
353 to subdivide the landscape into different functional units (plateaus, hillslopes, wetlands,  
354 rivers), and to represent each of them by a specific combination of conceptual model  
355 components to mimic their dominant runoff generation processes. Landscapes with different  
356 dominant runoff generation mechanisms are represented through an appropriate combination  
357 of these conceptual “building blocks” (Fencia et al., 2014; Gao et al., 2014; Wrede et al.,  
358 2015) using suitable topographical signatures such as “Height Above Next Drainage”  
359 (Gharari et al., 2011) to estimate their areal share. This is a clear advantage that facilitates  
360 model calibration and reduction of predictive uncertainty.

361 The strength of integral conceptual models is their ability to provide parsimonious and  
362 reliable predictions of streamflow  $Q$  ( $\text{m}^3 \text{s}^{-1}$ ) directly at the catchment outlet. However, it is  
363 nevertheless not straightforward to apply the models for predictions of transport of tracers,  
364 and more generally chemical species through the catchment into a stream, as elaborated in the  
365 following.

### 366 **2.2.3 Integral approaches to solute transport modelling in catchment hydrology**

367 Predictions of solute transport require information about the spectrum of fluid velocities  
368 and travel distances across the various flow paths into the stream (we can usually neglect the  
369 travel time within the river network due to the much higher fluid velocities, as argued in Sect.  
370 3.1). Such information can generally be inferred from breakthrough curves of tracers that  
371 enter and leave the system through well-defined boundaries, as shown for instance by the  
372 early work of Simmons (1982) and Jury et al. (1986), using transfer functions to model solute  
373 transport through soil columns. The transfer function approach is based on the theory of linear  
374 systems. This implies that the outflow concentration (volumetric flux-averaged concentration)

375  $C_{out}$  ( $\text{kg m}^{-3}$ ) at time  $t$  is, in case of steady-state water flow, the convolution of the solute  
376 input time series  $C_{in}$  with the system function  $G$  (Green's function):

377  
378 
$$C_{out}(t) = \int_0^{\infty} G(t - \tau) C_{in}(\tau) d\tau \quad (\text{Eq. 4})$$

379  
380 The transfer function is the system response to a delta function input. Note that Eq. 4  
381 should in general be formulated for the input and output mass flows, which correspond to the  
382 input/output concentration multiplied by the input/output volumetric water flows. It is  
383 important to note in this context is that the average travel time through the system can be  
384 calculated from the water flow and length of flow path, as the average travel velocity  
385 corresponds to the flow divided by the wetted cross section of the soil column (see Eq. 3). The  
386 latter implies that travel time distributions through partially saturated soils are transient and  
387 hence constrained by the input time (Jury et al., 1986; Sposito et al. 1986). The well-known  
388 fact that the flow velocity field changes continuously with changing soil water content  
389 explains why transfer function approaches have been largely put aside in soil physics and  
390 solute transport modelling in the partially saturated zone.

391 In the case of catchments, simulated runoff from conceptual hydrological models cannot,  
392 unfortunately, be used to constrain the average transport velocity. This is simply because  
393 conceptual models provide, by definition, no information about the wetted cross of the flow  
394 path through the catchment, and the latter determines essentially the average fluid velocity  $v$   
395 from simulated total runoff  $Q$ . The fact that the simple equation  $Q = v_{transport} A_{wet}$  has an  
396 infinite solution space, if  $A_{wet}$  is unknown, is also a major source of equifinality. This was  
397 shown by Klaus and Zehe (2010) and Wienhöfer and Zehe (2014), using a physically-based  
398 hydrological model to investigate the role of vertical lateral preferential flow paths of  
399 hillslope rainfall runoff response. These authors found that several network configurations  
400 matched the observed flow response equally well: some configurations consisted of a small  
401 number of larger macropores of higher conductance, while others consisted of a higher  
402 number of less conductive macropores. Overall, these configurations yielded the same  
403 volumetric water flow, but they performed rather differently with respect to simulation of  
404 solute transport. An even larger challenge for transport modelling through catchments arises  
405 from the fact that the distribution of flow path lengths is even more difficult to constrain,  
406 compared to a soil column.

407 Despite these challenges, the tracer hydrology community made considerable progress in  
408 understanding catchment transit time distributions and predicting isotope or tracer  
409 concentrations in streamflow (Harman, 2015). Initially, stable isotopologues of the water  
410 molecule and other tracers gained attention as they allow a separation of the storm hydrograph  
411 into pre-event and event water fractions using stable end member mixing (Bonell et al., 1990;  
412 Sklash et al., 1996). Today isotopes of the water molecules and water chemistry data are used  
413 as a continuous source of information to infer travel time distributions of water through  
414 catchments (McGlynn et al., 2002; McGlynn and Seibert, 2003; Weiler et al., 2003; Klaus et  
415 al., 2013). Early attempts to predict tracer concentrations in the stream relied on the same kind  
416 of transfer functions as outlined in Eq. (4) for soil columns. Hence, they naturally faced the  
417 same problems of state and thus time-dependent travel time distributions (Hrachowitz et al.,  
418 2013; Klaus et al., 2015; Rodriguez et al., 2018). More recent approaches rely on age ranked

419 storage as a “state” variable in combination with StoreAgeSelection (SAS) functions for  
420 stream flow and evapotranspiration to infer their respective travel time distributions (Harmann  
421 et al. 2015; Rinaldo et al., 2015). Aged ranked storage needs to be inferred from solving the  
422 Master equation, i.e., the catchment water balance for each time and each age. This can be  
423 done either by using conceptually modelled or observed discharge and evapo-transpiration,  
424 and it requires a proper selection of the functional form of the SAS functions and optionally  
425 their time-dependent weights (Rodriguez and Klaus, 2019). Related studies rely on a single or  
426 several gamma distributions (Hrachowitz et al., 2010; Klaus et al., 2015; Rodriguez and  
427 Klaus, 2019), others used the beta distribution (van der Velde et al., 2012) or piece-wise linear  
428 distributions (Hrachowitz et al., 2013, 2015).

429 Here we propose that the continuous time random walk (CTRW) framework from the  
430 groundwater “world” has much to offer to catchment travel time modelling (as detailed in  
431 Sect. 3). We show that, in particular, the inverse gamma distribution may offer a useful  
432 alternative that offers the asset of a clear connection to microscale physics and the well-  
433 known advection-dispersion equation, which is used in bottom up modelling (Sect. 2.2.4). In  
434 this context, it is interesting to recall that catchments were modelled as time-invariant linear  
435 systems for a considerable time, since the unit hydrograph was introduced by Sherman  
436 (1932). While the effect of precipitation was calculated using runoff coefficients, the  
437 streamflow response was simulated by convoluting effective precipitation with the system  
438 function, i.e., the unit hydrograph. The “Nash” cascade of linear reservoirs was a popular  
439 means to describe the unit hydrograph in a parametric form, and it is well known that the  
440 latter is mathematically equivalent to a gamma distribution (Nash, 1957). As streamflow  
441 response of the catchment is affected largely by surface and subsurface preferential pathways,  
442 which cause non-Fickian transport, one might hence wonder whether a gamma distribution  
443 function is an ideal choice to represent the fingerprint of preferential flow.

#### 444 **2.2.4 Bottom up modelling of the catchment water balance**

445 The blueprint of a physically based hydrological, introduced by Freeze and Harlan (1969),  
446 has found manifold implementations. Physically-based models like MikeShe (Refsgaard and  
447 Storm, 1995) or CATHY (Camporese et al., 2010) typically rely on the Darcy-Richards  
448 concept for soil water dynamics (Eq. 3), the Penman–Monteith equation for soil-vegetation-  
449 atmosphere exchange processes, and the Manning’s equation for estimating overland and  
450 stream flow velocities (Eq. 2).

451 Each of these approaches is naturally subject to limitations, reflecting our yet imperfect  
452 understanding, and suffers from the limited transferability of their related parameters from  
453 idealised, homogeneous laboratory conditions to heterogeneous and spatially organised  
454 natural systems (Grayson et al., 1992; Gupta et al., 2012). In this context, the Darcy-Richards  
455 model receives by far the strongest criticism (Beven and Germann, 2013), simply because the  
456 underlying assumption regarding the dominance of capillarity-controlled diffusive flow, under  
457 local equilibrium conditions, is largely inappropriate when accounting for preferential flow.  
458 The Darcy model is hence incomplete when accounting for infiltration (Germann, 2018) and  
459 preferential flow, and several approaches have been proposed to close this gap. These range  
460 from the early idea of (a) stochastic convection assuming no mixing at all (Simmons, 1982),  
461 to (b) dual-permeability conceptualizations relying on overlapping, exchanging continua

462 (Šimunek et al., 2003), to (c) spatially explicit representations of macropores as connected  
463 flow paths (Vogel et al., 2006; Sander and Gerke, 2009; Zehe et al., 2010; Wienhoefer and  
464 Zehe, 2014; Loritz et al., 2017), and to (d) pore-network models based on mathematical  
465 morphology (Vogel and Roth, 2001). An alternative approach to dealing with preferential  
466 flow and transport employs Lagrangian models such as SAMP (Ewen, 1996a,b), MIPs  
467 (Davies and Beven, 2012; Davies et al., 2013), and LAST (Zehe and Jackisch, 2016; Jackisch  
468 and Zehe, 2018; Sternagel et al., 2019).

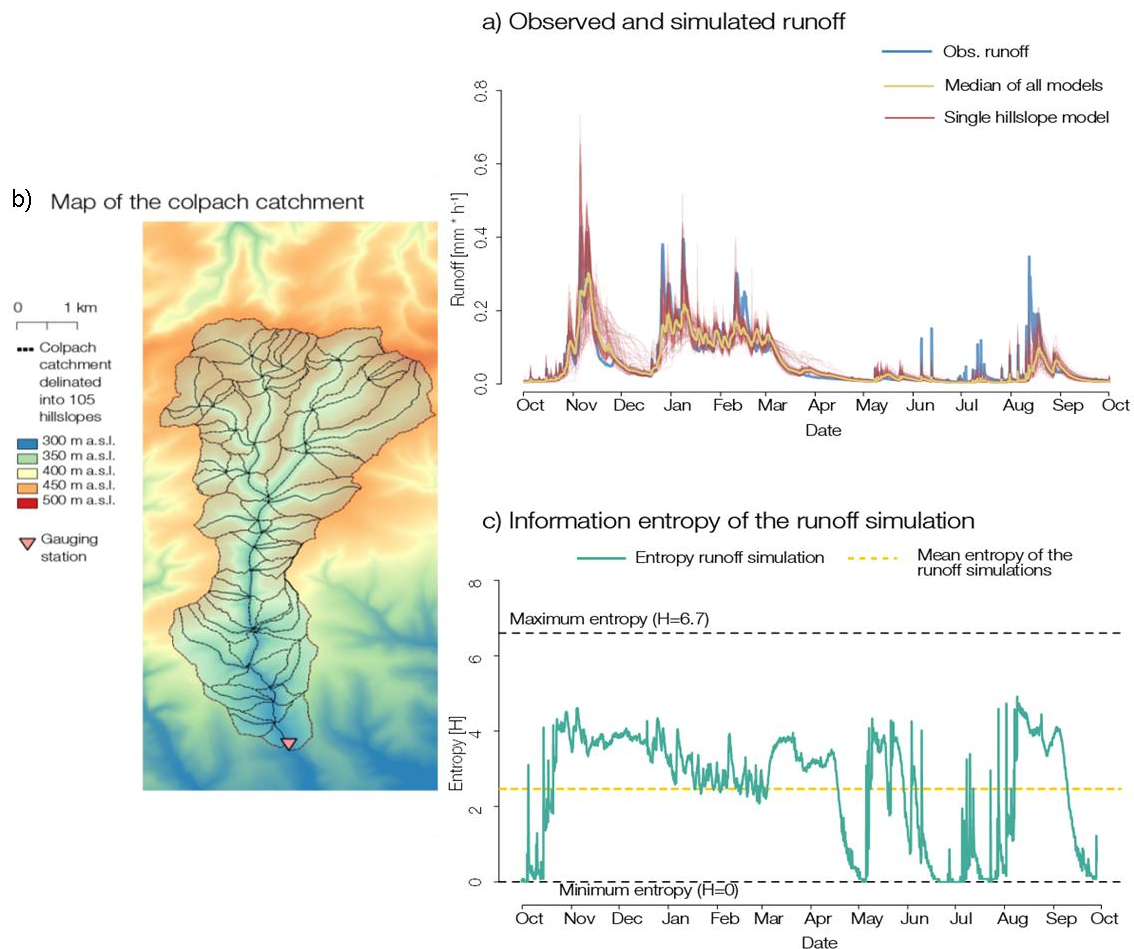
469 Reductionist models are, despite the challenge to represent preferential flow and transport,  
470 indispensable tools for scientific learning. They particularly allow exploration of how  
471 distributed patterns and their spatial organisation jointly controls distributed state dynamics  
472 and integral behaviour of hydrological systems (Zehe and Blöschl, 2004). Related studies  
473 range from, e.g., the investigation of (a) how changes in agricultural practices affect the  
474 stream flow generation in a catchment (Pérez et al., 2011), (b) the role of bedrock topography  
475 for runoff generation using (Hopp and McDonnell; 2009) at the Panola hillslope and the  
476 Colpach catchment (Loritz et al. 2017), or (c) the role of vertical and lateral preferential flow  
477 networks on subsurface water flow and solute transport at the hillslope scale (Bishop et al.,  
478 2015; Wienhöfer and Zehe; 2014; Klaus and Zehe; 2011; Klaus and Zehe, 2010), including  
479 the issue of equifinality. Setting up a physically-based model, however, requires an enormous  
480 amount of highly resolved spatial data, particularly on subsurface characteristics. Such data  
481 sets are rare, and the “hunger” for data in such models risks a much higher structural model  
482 uncertainty. On the other hand, these models offer also greater opportunities for constraining  
483 their structure using multiple data orthogonal to discharge (Ebel and Logue, 2006; Wienhöfer  
484 and Zehe, 2014).

485 Another asset of reductionist models is their thermodynamic consistency, which implies  
486 that energy conversions related to flow and storage dynamics of water in the catchment  
487 systems are straightforward to calculate (Zehe et al, 2014). This offers the opportunity to test  
488 the feasibility of thermodynamic optimality as constraint for parameter inference (Zehe et al.;  
489 2013), the latter is rather challenging when using conceptual (Westhoff et al., 2013, Westhoff  
490 et al., 2016). More recent applications demonstrated, in line with this asset, new ways to  
491 simply distributed models without lumping, which allowed the successful simulation of the  
492 water balance of a 19 km<sup>2</sup> large catchment using a single effective hillslope model (Loritz et  
493 al., 2017). The key to this was to respect energy conservation during the aggregation  
494 procedure, specifically through derivation of an effective topography that conserved the  
495 average distribution of potential energy along the average flow path length to the stream; and  
496 through a macroscale effective soil water retention curve that conserved the relation between  
497 the average soil water content and matric potential energy using a set point scale retention  
498 experiments (Jackisch 2015; Zehe et al., 2019).

499 Along similar lines, Loritz et al. (2018) showed that simulations using a fully distributed  
500 setup of the same Colpach catchment using 105 different hillslopes yielded strongly  
501 redundant contributions of stream flow (Fig. 2). They used the Shannon entropy (Shannon,  
502 1948, defined in Eq. 6 in section 2.4) to quantify the diversity in simulated runoff of the  
503 hillslope ensemble at each time step. They found that although the entropy of the ensemble  
504 was rather dynamic in time, it never reached the maximum value. Note that an entropy  
505 maximum implies that hillslopes contribute in a unique fashion, while a value of zero implies

506 that all hillslope yield a similar runoff response. They further showed that the fully distributed  
 507 model, consisting of 105 hillslopes, can be compressed to a model using 6 hillslopes with  
 508 distinctly different runoff responses, without a loss in simulation performance. Based on these  
 509 findings, they concluded that spatial organisation leads to emergence of functional similarity  
 510 at the hillslope scale, as proposed by Zehe et al. (2014). This in turn explains why conceptual  
 511 models can be reasonably applied as most of the spatial heterogeneity in the catchment seems  
 512 to be irrelevant for runoff production. However, this is not the case, when it comes to  
 513 transport of chemicals as elaborated in the next section.

514 In accord with Hrachowitz and Clark (2017), we conclude that top down and bottom up  
 515 models indeed have complementary merits. Moreover, we propose that the applicability of  
 516 conceptual models at larger scales arises from the fact that spatial organisation leads in  
 517 conjunction with the strongly dissipative nature of hydrological process to the emergence of  
 518 simplicity at larger scales (Savenije and Hrachowitz, 2017; Loritz et al., 2018).  
 519



520  
 521 **Figure 2** (a) Observed and simulated runoff of the Colpach catchment. The red lines  
 522 correspond to individual hillslope models and the yellow line to area weighted median of all  
 523 hillslopes. (b) Map of the Colpach catchment and the 105 different hillslopes. (c) Shannon  
 524 entropy in turquoise for the runoff simulations as well as the corresponding mean. © Ralf  
 525 Loritz KIT, from Loritz et al. (2018).

## 526 **2.3 Distributed solute transport modelling – the key role of the critical zone**

527 Reductionist physically models are straightforwardly to couple with the advection-  
528 dispersion equation (compare Eq. 11 in Sect. 3) or particle tracking schemes to simulate  
529 transport of tracers and reactive compounds through the critical zone into groundwater or  
530 along the surface and through the subsurface into the stream.

531 The soil-vegetation-atmosphere-transfer system (SVAT-system), or in more recent terms,  
532 the “critical” zone, is the mediator between the atmosphere and the two water worlds. This  
533 tiny compartment controls the splitting of rainfall into overland flow and infiltration, and the  
534 interplay among soil water storage, root water uptake and groundwater recharge. Soil water  
535 and soil air contents control CO<sub>2</sub> emissions of forest soils, denitrification and related trace gas  
536 emissions into the atmosphere (Koehler et al. 2010; Koehler et al, 2012), as well as  
537 biogeochemical transformations of chemical species.

538 Partly saturated soils may, depending on initial their state and structure, respond with  
539 preferential flow and transport of contaminants and nutrients through the biological most  
540 active topsoil buffer (Flury et al., 1994, 1995; Flury, 1996; McGrath et al., 2008, 2010; Klaus  
541 et al., 2014). Rapid transport operates within strongly localized preferential pathways such as  
542 root channels, cracks, worm burrows or within connected inter-aggregate pore networks  
543 which “bypass” of the soil matrix continuum (e.g., Beven and Germann, 1982; Blume et al.,  
544 2009; Wienhöfer et al., 2009; Beven and Germann, 2013). The well-known fingerprint of  
545 preferential flow is a “fingered” flow pattern, which is often visualised through dye staining  
546 or two-dimensional concentration patterns in vertical soil profiles (Fig. 3). These reveal  
547 imperfectly mixed conditions in the near field, which implies that the spatial concentration  
548 pattern deviates from the well mixed Fickian limit over a relatively long time. The latter  
549 corresponds in the case of a delta input to a Gaussian distribution of travel distances at a fixed  
550 time, where the centre of mass travels with the average transport velocity while the spreading  
551 of the concentration grows linearly with time proportional to the macrodispersion coefficient  
552 (Simmons, 1982; Bodin, 2015). Note that according to Trefry et al. (2003), this Gaussian  
553 travel distance corresponds to a state of maximum entropy. Preferential flow hence implies a  
554 deviation from this well mixed maximum entropy state, which cannot be predicted with the  
555 advection-dispersion equation (e.g., Roth and Hammel, 1996). A recent study (Sternagel et  
556 al., 2019) revealed that even double domain models such as Hydrus 1D may fail to match the  
557 flow fingers and/or long-time concentration tails in tracer profiles. Frequently, the partially  
558 saturated region of the subsurface is simply too thin to allow perfectly mixed Gaussian travel  
559 distances to be established; hence non-Fickian transport in the critical zone is today regarded  
560 as being the rule rather than the exception.

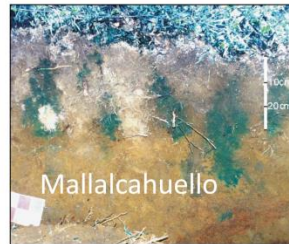
561



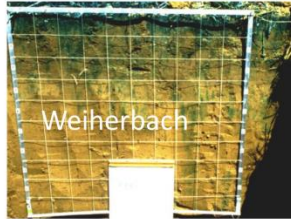
Germany, van Schaik et al. (2014)



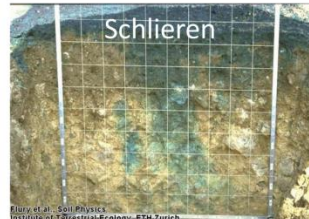
Chile, Blume et al. (2009) Austria, Wienhöfer et al. (2009)



Germany, Zehe and Flüher (2001)



Switzerland, Flury et al. (1994)



562  
563  
564  
565  
566  
567  
568  
569  
570

**Figure 3** Finger flow pattern revealed from standardized dye staining experiments for a transport time of 1 day; images were generously provided by Flury et al. (2004; 2005; Copyright © 1994, 1995 the American Geophysical Union) for Switzerland, Blume et al. (2009, Copyright © Theresa Blume) for Chile, Wienhöfer et al. (2009, Copyright © Jan Wienhöfer KIT) for Austria, and Zehe and Flüher (2001, Copyright © Erwin Zehe KIT) and van Schaik et al. (2014, Copyright © 2013 John Wiley & Sons, Ltd.) for the German Weierbach.

571 Because preferential transport leads to strongly localized accumulation of water and  
572 chemical species, preferential pathways are potential biogeochemical hotspots. This is  
573 particularly the case for biopores such as worm burrows and root channels. Worm burrows  
574 provide a high amount of organic carbon and worms “catalyse” microbiological activity due  
575 to their enzymatic activity (Bundt et al., 2001; Binet et al., 2006; Bolduan and Zehe, 2006;  
576 van Schaik et al., 2014). Similarly, plant roots provide litter and exude carbon substrates to  
577 facilitate nutrient uptake. Intense runoff and preferential flow events optionally connect these  
578 isolated “hot spots” to lateral subsurface flow paths such as a tile drain network or a pipe  
579 network along the bedrock interface, and thereby establish “hydrological connectivity”  
580 (Tromp-van Meerveld and McDonnell, 2006; Lehmann et al., 2007; Faulkner, 2008). The  
581 onset of hydrological connectivity comprises again a “hot moment” as upslope areas and,  
582 potentially, the entire catchment start “feeding” the stream with water, nutrients and  
583 contaminants (Wilcke et al., 2001; Goller et al., 2006).

584 The critical zone, furthermore, crucially controls the Bowen ratio (the partitioning of net  
585 radiation energy into sensible and latent heat), and soil water available to plants is a key  
586 controlling factor. The residual soil water content is not available for plants, as it is generally  
587 stored in fine pores subject to very high capillary forces. Isotopic tracers have been  
588 fundamental to unravelling water flow paths in soils, using dual plots (Benettin et al., 2018;  
589 Sprenger et al., 2018), and to distinguish soil water that is recycled to the atmosphere and  
590 released as stream flow (Brooks et al., 2010; McDonnell, 2014).

591 Further to the above points, it is noted that laboratory and numerical studies of multiple  
592 cycles of infiltration-drainage of water and chemicals into a porous medium demonstrate  
593 clearly the establishment of stable “old” water clusters/pockets, and even a “memory effect”  
594 (Kapetas et al., 2014), which remain even with multiple cycles of “new” water infiltration  
595 (Gouet-Kaplan and Berkowitz, 2011). These pore-scale studies are in qualitative (and semi-  
596 quantitative) agreement with studies at the *field scale*, which show similar retention behaviour  
597 of bromide (introduced during the first infiltration cycle) after multiple infiltration-drainage  
598 cycles (Turton et al., 1995; Collins et al., 2000). As a consequence, when each cycle of  
599 infiltration contains water with a different chemical signature, stable pockets of water can be  
600 established with highly varying chemical composition. We hence emphasise that mobile and  
601 immobile waters sustaining evaporation and stream flow – and the chemical species they  
602 contain – exist at a continuum of scales from the pore to the field level. Thus, rather than  
603 attempting to delineate pockets of less and more mobile water at each scale – separating these  
604 pockets at the pore, the column, the meter, the 10 meter, and the field and catchment scales –  
605 we instead suggest recognising and delineating an “overall effect” of separation between  
606 “old” (immobile) and “new” (mobile) waters at a given “effective” scale of interest, which  
607 integrates over all such old and new waters. As we discuss in detail at the end of Sect. 3.1, and  
608 thereafter, then, we argue that it is a more effective approach to consider chemical transport as  
609 following *distributions of travel distances and residence times*, which can then be characterized  
610 by various (often power law) probability density functions.

## 611 **2.4 Groundwater systems**

612 As noted in Sect. 1, analysis of groundwater systems has developed largely independently  
613 of investigation of catchment systems, although it, too, developed originally as a large  
614 deterministic engineering discipline around the traditional task of water supply for domestic  
615 and agricultural use. It was only in the 1980’s that “stochastic” (probabilistic and statistical)  
616 techniques began to be implemented extensively, to account for the many uncertainties  
617 associated with aquifer structure and hydraulic properties that control the flow of  
618 groundwater. In parallel, significant interest (and concern) with water quality and  
619 environmental contamination in groundwater systems only entered the research community’s  
620 consciousness in the 1980s, although some pioneering laboratory experiments and field  
621 measurements were initiated from the late 1950s.

622 It is worth noting, too, that the methods and models applied in groundwater research  
623 developed independently and separately from research on catchment systems (Sect. 1). The  
624 only partial connection or “integrator” has traditionally been with aquifer connections to the  
625 vadose zone (or critical zone, discussed in Sect. 2.3). Another connection between surface  
626 water and groundwater systems, though not generally recognized as such, has been analysis of  
627 water flow, and to a lesser extent chemical species transport, in the hyporheic zone. The  
628 hyporheic zone can be defined as the region of sediment and subsurface porous domain below  
629 and adjacent to a streambed, which enables mixing of shallow groundwater and surface water.  
630 (e.g., Haggerty et al, 2002).

631 To quantify chemical transport, landmark laboratory experiments (e.g., Aronofsky and  
632 Heller, 1957; Scheidegger, 1959) measured breakthrough of conservative (non-reactive)  
633 chemical tracers through columns of sand. These measurements underpinned theoretical



634 developments, based also on concepts of Fickian diffusion, which led to consideration of the  
635 classical advection-dispersion equation. Since that time, the advection-dispersion equation –  
636 and variants of it – have been used extensively to quantify chemical transport in porous  
637 media. However, as thoroughly discussed in Berkowitz et al. (2006), solutions of the  
638 advection-dispersion equation have repeatedly demonstrated an inability to properly match  
639 results of extensive series of laboratory experiments, field measurements, and numerical  
640 simulations. These findings naturally lead to the conclusion that the conceptual picture  
641 underlying the advection-dispersion equation framework is insufficient; as detailed in Sect.  
642 2.2, the soil physics community arrived at a similar conclusion. Stochastic variants of the  
643 advection-dispersion equation, and implementation of multiple-continua, advection-dispersion  
644 equation formulations (including mobile-immobile models) have been used to provide  
645 insights into factors that affect chemical transport – particularly given uncertain knowledge of  
646 detailed structural and hydraulic aquifer properties – but they have been largely unable to  
647 capture measured behaviours of chemical transport. This observation is largely in line with  
648 what we reported for the critical zone.

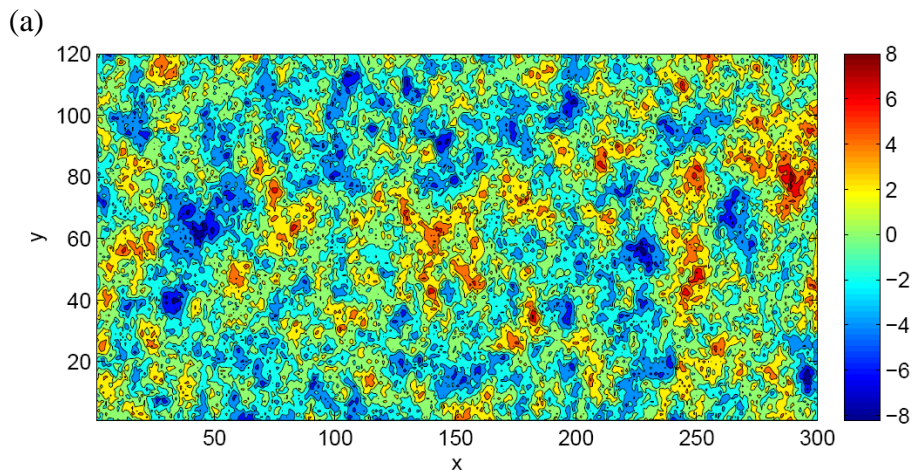
649 The first key is to recognize that heterogeneities are present at all scales in groundwater  
650 systems, from sub-millimetre pore scales to the scale of an entire aquifer. Indeed, use of the  
651 term “heterogeneities” refers to varying distributions of structural properties (e.g., porosity,  
652 presence of fractures and other lithological features), hydraulic properties (e.g., hydraulic  
653 conductivity), and – in the case of chemical transport (a general term used here and  
654 throughout to denote migration of chemical (and/or microbial) components) – variations in  
655 the biogeochemical properties of the porous domain medium. The second key is to recognize  
656 that these variations in distributions, at all scales, deny the possibility of obtaining complete  
657 knowledge of the aquifer domain in which fluids and chemical species are transported. A third  
658 key, when considering chemical transport (and transport of stable water molecule isotopes), is  
659 to recognize that chemical species are subject to several critical transport mechanisms and  
660 controls, in addition to advection, that do not affect flow of water – molecular diffusion,  
661 dispersion, and reaction (sorption, complexation, transformation) – so that chemical migration  
662 through an aquifer is influenced strongly by aquifer heterogeneities and initial/boundary  
663 conditions. Extensive analysis of high-resolution experimental measurements and numerical  
664 simulations of transport demonstrate that small-scale heterogeneities can significantly affect  
665 large-scale behaviour, and that small-scale fluctuations in chemical concentrations do not  
666 simply average out and become insignificant at large scales.

667 As discussed in the preceding sections, preferential pathways are ubiquitous and affect  
668 both water and chemical species, resulting from system heterogeneity. To be more specific,  
669 (local) hydraulic conductivities vary in space over orders of magnitudes, even within  
670 distances of centimetres to meters, and these variations ultimately control patterns of fluid and  
671 chemical movement. The resulting patterns of movement in these systems involve highly  
672 ramified preferential pathways for water movement and chemical migration. To illustrate  
673 these points, consider the hydraulic conductivity ( $K$ ) and preferential pathway maps shown in  
674 Fig. 4a; see Edery et al. (2014) for full details.

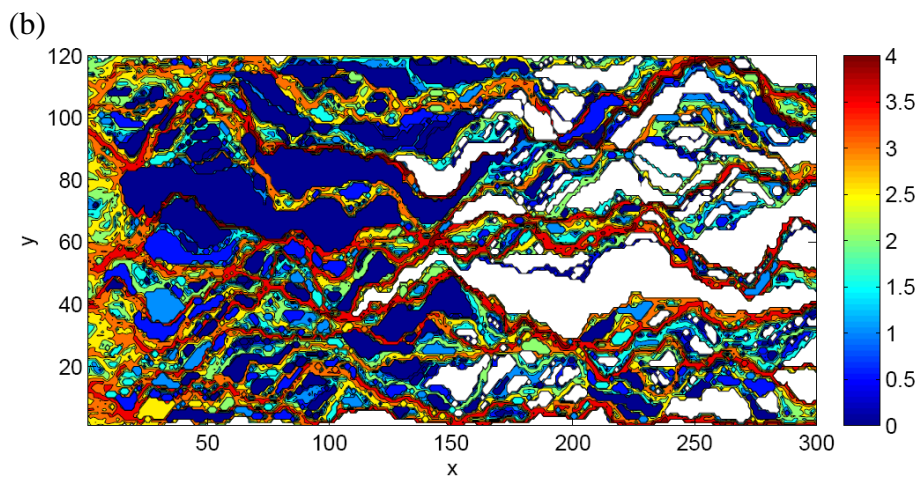
675 Figure 4a shows a numerically-generated, two-dimensional domain measuring  $300 \times 120$   
676 discretized into grid cells of uniform size (0.2 units). The  $K$ -field shown here was generated as  
677 a random realization of a statistically homogeneous, isotropic, Gaussian  $\ln(K)$  field, with

678  $\ln(K)$  variance of  $\sigma^2 = 5$ . Fluid flow through this domain was solved at the Darcy level by  
679 assuming constant head boundary conditions on the left and right boundaries, and no-flow  
680 horizontal boundaries; the hydraulic head values determined throughout the domain were then  
681 converted to local velocities, and thus streamlines. Conservative chemical transport was  
682 determined using a standard Lagrangian particle tracking method, with  $10^5$  particles  
683 representing the dissolved chemical species. Particles advanced by advection along the  
684 streamlines and molecular diffusion (enabling movement between streamlines), to generate  
685 breakthrough curves (concentration vs. time) at various distances along the domain. Figure 4b  
686 shows particle pathways through the domain, wherein the number of particles visiting each  
687 cell is represented by colours. The emergence of distinct, limited particle preferential  
688 pathways from inlet boundary to outlet boundary is striking. Notably, too, there are significant  
689 regions that remain free of particles (the white regions in Fig. 4b), and preferential pathways  
690 are confined and converge between low conductivity areas. Even more striking is set of even  
691 sparser preferential pathways shown in Fig. 4c: here, only cells, which were visited by at least  
692 0.1% of all injected particles, are shown. In other words, 99.9% of all chemical species  
693 migrating through the domain shown in Fig. 4a advance through a limited number and spatial  
694 extent of preferential pathways. It is significant, too, that the preferential pathways comprise a  
695 combination of higher conductivity cells the paths, but also some low conductivity cells, as  
696 reported also in Bianchi et al. (2011); see Sect. 3.1 for further discussion of this behaviour.

697  
698  
699

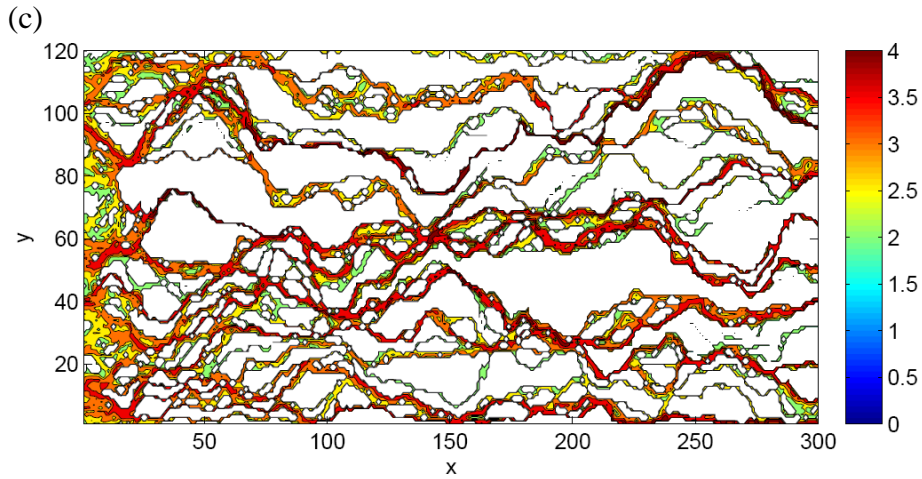


700  
701



702

703

704  
705

706 **Figure 4 (a)** Spatial map showing a sample hydraulic conductivity ( $K$ ) field generated  
 707 statistically (right side bar shows scale of  $\ln(K)$ ). **(b)** Spatial map showing particle paths  
 708 through the domain, for overall hydraulic gradient (water flow) from left to right. “Particles”  
 709 representing dissolving chemical species are injected along the left vertical boundary and  
 710 followed through the domain. White regions indicate where *no* particles “visit” (interrogate)  
 711 the domain. Blue regions have only a small number of particle visitations. Red regions have  
 712 significant particle visitations. Note that the colour bar is in  $\log_{10}$  number of particles. **(c)**  
 713 Spatial map showing particle paths *preferential* particle paths, defined as paths through cells  
 714 (underlying subdivisions in the domain, each with a different  $K$  value as shown in plot (a)  
 715 above) that each contain a “visitation” of a minimum of 0.1% of the total number of particles  
 716 in the domain. Note that the colour bar is in  $\log_{10}$  number of particles (after Edery et al.,  
 717 2014; Copyright 2014, with permission from the American Geophysical Union).

718

719 Thus, it is clear that the groundwater systems incorporate regions of water – distributed  
 720 throughout the domain – that may have very different chemical signatures, even in close  
 721 proximity to each other. Moreover, these regions can be relatively stable over time, modified  
 722 only by the extent of chemical diffusion into and out of the “immobile” regions.

723 In accord with our definition of spatial organisation in Sect. 1, we propose the use of  
 724 Shannon entropy  $H$  (bits) to quantify the degree of spatial organisation in the flow pattern in  
 725 Fig. 4c. To this end, we define the discrete probability density distribution to find a particle in  
 726 a grid element,  $\Delta y_i$ , at the inlet ( $x=0$ ) and at the outlet ( $x=300$ ) of the flow domain, based on  
 727 the numbers of particles that entered/left the domain through the corresponding grid cells  
 728 divided the total number of particles that entered/left the domain  $N_{in}/N_{out}$ , as follows:

729

$$730 \quad p(x=0, \Delta y_i) = \frac{n(\Delta y_i, x=0)}{N_{in}}; \quad p(x=300, \Delta y_i) = \frac{n(\Delta y_i, x=300)}{N_{out}} \quad (\text{Eq. 5})$$

731

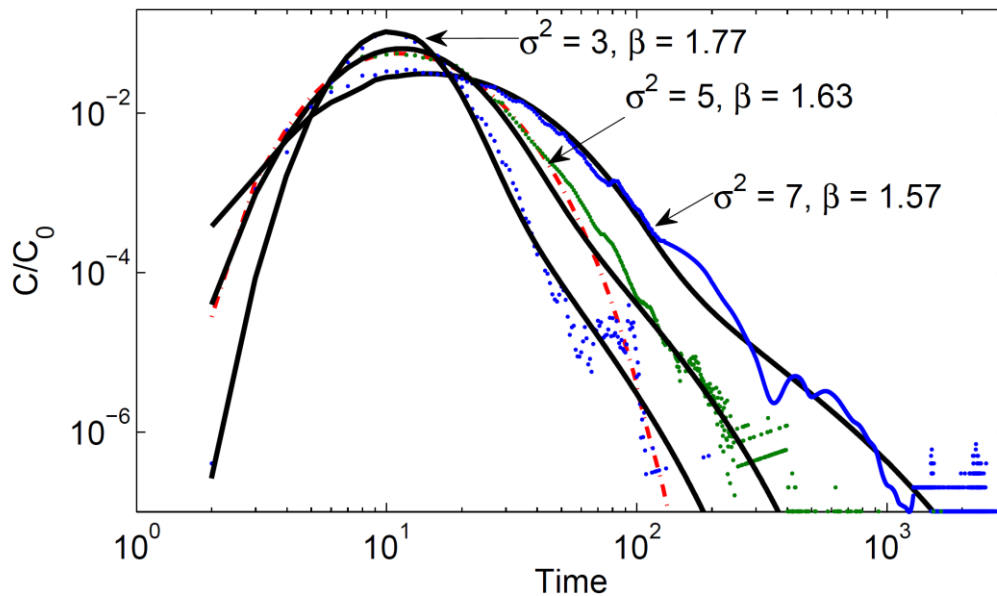
732 where  $p(x=0, \Delta y_i)/p(x=300, \Delta y_i)$  are probabilities that particle entered/left the domain at  $\Delta y_i$ ,  
 733  $n(x=0, \Delta y_i)/n(x=300, \Delta y_i)$  are the numbers of particles that entered/left the domain at  $\Delta y_i$ .  
 734 Using these probability distributions, we calculate the respective Shannon entropy values  
 735 defined as follows:

736

$$736 \quad H = -\sum p_i \log_2(p_i) \quad (\text{Eq. 6})$$

737

738 The Shannon entropy of the uniform input distribution, with 6.9 bits, corresponds to an  
 739 entropy maximum. Preferential flow reduced this to  $H = 3.58$  bits at the outlet, which reflects  
 740 a release of chemicals that is much more organised in space. Note that a well-mixed  
 741 advective-dispersive pattern would maximise the entropy at the outlet, as the concentration  
 742 would be constant along the  $y$  coordinate. Considering now arrival times of chemical species  
 743 at the domain outlet boundary, Fig. 5 shows the relative concentration ( $C/C_0$ ) vs. time –  
 744 breakthrough curves – for three degrees of domain heterogeneity ( $\ln(K)$  variance). (The well-  
 745 mixed case would maximise the entropy at the outlet, corresponding to a CTRW fit with  $\beta = 2$   
 746 in Fig. 5.) It is evident that the chemical transport in this domain displays “non-Fickian” (or  
 747 “anomalous”) transport, in the sense that late-time (long tail) arrivals are registered at the  
 748 measurement plane. Furthermore, Fickian-based advection-dispersion equation models clearly  
 749 fail to quantify such behaviour (Fig. 5). However, Fig. 5 shows solutions – based on the  
 750 continuous time random walk (CTRW) framework – that do effectively describe the chemical  
 751 transport. The CTRW framework and governing transport equations are detailed in Sect. 3.3.  
 752  
 753



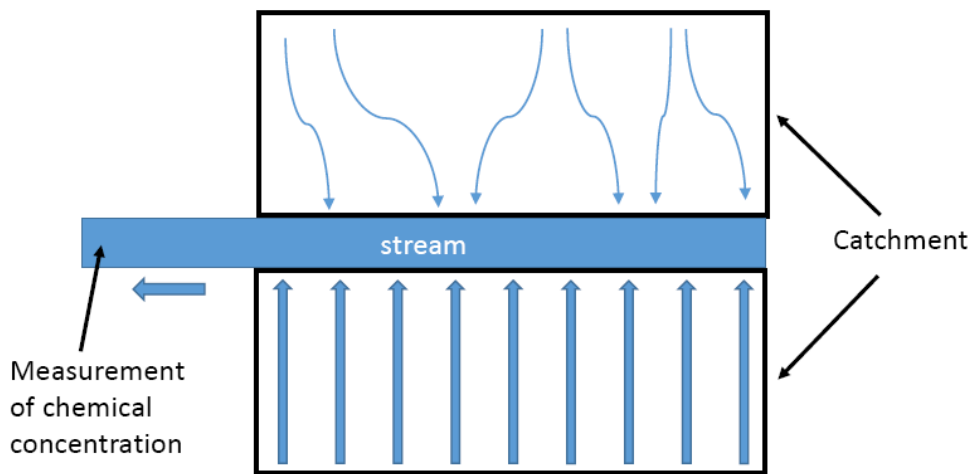
754  
 755 **Figure 5** Breakthrough curves (points) for three  $\ln(K)$  variances ( $\sigma^2 = 3, 5, 7$ ; 100 realizations  
 756 each), at the domain outlet ( $x = 300$  length units), and corresponding CTRW fits (curves).  
 757 Also shown is a fit of the advection-dispersion equation (dashed-dotted curve), for  $\sigma^2 = 5$ .  
 758 See Sect. 3.3 for further discussion and explanation of  $\beta$ . All values are in consistent, arbitrary  
 759 length and time units (after Ederly et al., 2014; Copyright 2014, with permission from the  
 760 American Geophysical Union).

### 761 3 MERGING TREATMENT OF SURFACE WATER AND 762 GROUNDWATER SYSTEM TRANSPORT DYNAMICS

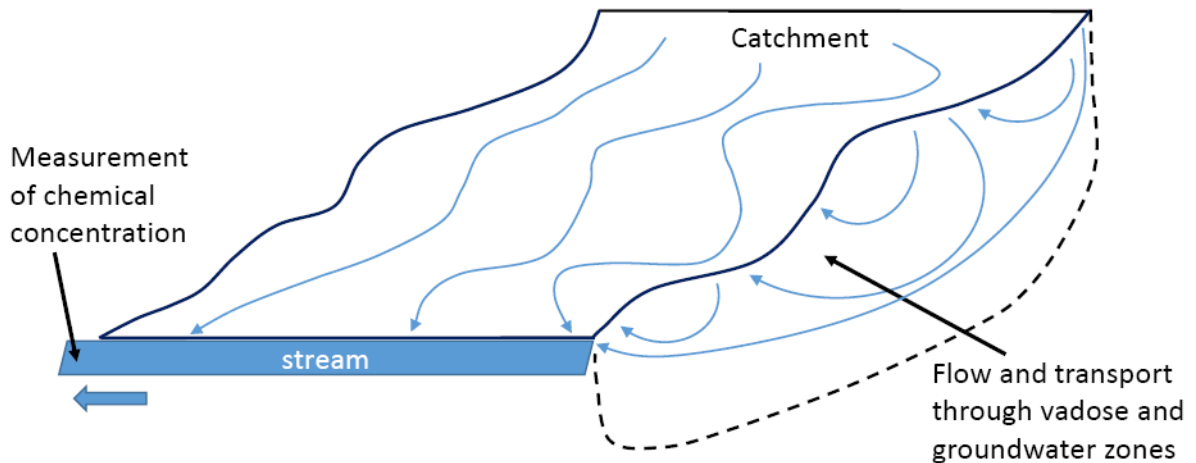
#### 763 3.1 Conceptual pictures, travel times, and mixtures of water with different chemical 764 signatures

765 Clearly, any quantitative model of fluid flow and chemical transport in a catchment must  
 766 first define a conceptual picture. In the context of the discussion in Sects. 2 and 3 that led us

767 to this point, we require a picture that accounts naturally for overland and interacting  
 768 subsurface flow and transport, recognizing the ubiquity of preferential pathways and a broad  
 769 (and often different) distributions of fluid and chemical travel times. Moreover, any such  
 770 conceptual picture also requires definition of the available measurement benchmark against  
 771 which a quantitative model can be compared. In the case of catchments, a common  
 772 measurement is that of chemical arrival times at a downstream sampling point in a catchment  
 773 stream that drains and exits the catchment. Thus, the dynamics of fluid flow and chemical  
 774 transport in a fully three-dimensional (or simplified two-dimensional overland) catchment  
 775 are often represented by measurements in an effective, spatially averaged one-dimensional  
 776 system. (Of course, higher resolution, multidimensional (in space) measurements, if available,  
 777 should also be considered in a quantitative model!)



779  
 780 (a)  
 781



782  
 783 (b)  
 784

785 **Figure 6** Conceptual pictures of water flow and chemical transport in catchments under a  
 786 pulse of rainfall over the entire catchment. Each curved arrow (or idealized straight arrow)  
 787 indicates a different path, each of which embodies different travel times through the system  
 788 until reaching the stream. Note that each preferential pathway carrying water and chemical



789 species may be purely overland, or include interactions and advance within soil layers  
790 (partially saturated, or vadose, zone) and saturated groundwater systems. **(a)** Schematic  
791 showing idealized 2D catchment area. Arrows through two rectangular regions of catchment  
792 indicate a range of preferential pathways carrying water and chemical species. **(b)** Schematic  
793 showing idealized 3D catchment area, under a pulse of rainfall over the entire catchment.  
794

795 Figures 6a and 6b show, schematically, 2D and 3D conceptualizations of preferential  
796 pathways, with associated varying travel times through the catchment, for both fluid flow and  
797 chemical transport. We stress here – and as discussed below in Sect. 3.3 – that the larger  
798 scale, effective (or “characteristic”, or average) fluid velocities and chemical species transport  
799 velocities need not be identical. For example, using a conceptual mixing model, Hrachowitz  
800 et al. (2015) showed that chloride transport can be slower than water transport. In fact, these  
801 two velocities are rarely the same, as a consequence of the ubiquity of preferential pathways  
802 for water and migrating chemical species in any surface water and/or soil-aquifer domain.  
803 Because of these pathways, regions of higher and lower hydraulic conductivity (fluid and  
804 chemical mobility) – and thus the entire system – interrogated by water and chemical species  
805 differ. While both water molecules and chemical species are subject to diffusive and  
806 dispersive transport mechanisms, in addition to advection, these effects are clearly identifiable  
807 for chemical species, while they are undistinguishable for individual water molecules. Thus  
808 the effects of diffusion and dispersion on “bulk water” transport, e.g., into and out of low  
809 conductivity zones, are invisible and irrelevant, while chemical species retained in these same  
810 zones can have a major impact on the overall (and “average”, centre of mass) advance of a  
811 chemical plume. These effects are also visible and relevant for isotopes of the water molecule,  
812 as deuterium and tritium are subject to self-diffusion in water. The latter implies that isotope  
813 concentrations between old and new water pockets in the subsurface might mix diffusively,  
814 even when there is no physical mixing between these waters. Hence, the relation between  
815 water age and its isotopic decomposition is not straightforward.

816 The conceptual picture discussed here is our basis for arguing that we should expect to  
817 find distributions of travel times and mixtures of water with different chemical signatures, *at*  
818 *all scales*. Moreover, these considerations align well with our reflections in Sect. 2 and key  
819 studies in catchment hydrology, which clearly recognize the occurrence of wide distributions  
820 of water and chemical travel times, and long-term chemical persistence in water catchment  
821 storage (e.g., Niemi, 1977; Botter et al., 2010, 2011; Hrachowitz et al., 2010; McDonnell and  
822 Beven, 2014; Kirchner, 2016).

823 As pointed out in Sect. 2, several studies in recent years have specifically reported the  
824 presence of water bodies (or pockets, or regions, depending on scale), with different chemical  
825 compositions and isotopic signatures, that are in close proximity or even “overlapping” (in  
826 some sense). Some authors use the term “two water worlds” – immobile and mobile – in this  
827 context (e.g., McDonnell, 2014) to describe the different sources of water returned to the  
828 atmosphere by vegetation transpiration and released to streams; we stress again that our use of  
829 the term in this paper highlights the different catchment hydrology and groundwater  
830 communities and associated research tools. In light of the discussion in Sect. 2, we stress here  
831 that the conceptual picture to explain spatially and temporally varying chemical compositions  
832 (in subsurface, soil, sediment and aquifer systems), and associated uptake by vegetation, is  
833 subtle. We question the conceptualization of two (or more) *separate, fully compartmentalized*

834 mobile and immobile regions of water and chemicals. We argue that mobile and immobile  
835 regions are more appropriately considered as overlapping continua or ensemble/effective  
836 averages, as those are found at all scales from pores to hundreds of meters (e.g., Turton et al.,  
837 1995; Collins et al., 2000; Gouet-Kaplan and Berkowitz, 2011; recall Sect. 2.3). With the  
838 occurrence of mixtures of travel times and waters having different chemical signatures at all  
839 scales, we argue that it is preferable to think in terms of time, such that there is a range of  
840 overlapping temporal (transition time) distributions that each contribute to the overall, large-  
841 scale fluid flow and chemical transport. This leads naturally to the CTRW framework.

### 842 **3.2 Space vs. time: the travel time perspective of transport**

843 It is critical to point out that in the figures shown above in Sects. 2.3 and 2.4, the  
844 *residence times* of water and chemicals are the key factors that determine transport behaviour.  
845 This leads to the continuous time random walk (CTRW) framework, which operates more (or  
846 at least equally!) in terms of time than in terms of space (see Sect. 3.2). To introduce CTRW,  
847 in the context of the pathway “self-organisation” shown in Fig. 5c, we demonstrate the  
848 importance of thinking in terms of *time* rather than *space*. Consider the simple example of  
849 driving a distance of 100 km; we consider a scenario in which we travel 50 km at 1 km/h, and  
850 then 50 km at 99 km/h. The average speed of travel, in terms of *space* (distance), is  
851 determined as follows: given that we travelled 50 km at each of two speeds, the average speed  
852 is  $(1 + 99) / 2 = 50$  km/h. Thus, with this calculation, the total time to travel 100 km “should”  
853 be 2 h. However, the *actual* time taken to travel this distance – 50 km at 1 km/h, and then 50  
854 km at 99 km/h – is 50.5 h. In other words, traditional (but incorrect!) conceptual spatial  
855 thinking highlights the erroneous effects of focusing only on *spatial* heterogeneity and  
856 quantification based only on spatial characteristics.

857 In a similar analogy, it is sometimes faster to pass through a bottleneck region (e.g., drive  
858 for a short time through a very narrow and slow road) to ultimately reach a fast highway,  
859 rather than to travel at medium speed along a road for an entire journey.

860 Another aspect related to misplaced emphasis on spatial heterogeneities, is also noted  
861 here. Referring again to the preferential pathways show in Fig. 4c, it is seen that these  
862 pathways actually contain some low hydraulic conductivity ( $K$ ) regions as well! This can be  
863 explained most easily, conceptually, in terms of one-dimensional pathways. Consider a  
864 number of high and low  $K$  cells in series, [3 3 3 3 3] vs. [6 6 1 6 6], where the  
865 effective/average  $K$  is given by the harmonic mean. While a [3 3 3 3 3] series may appear to  
866 enable a greater volumetric flow rate than a [6 6 1 6 6] series, due to the “bottleneck” low  $K$   
867 value in the centre, both series in fact have the same harmonic mean ( $=3$ ) and conduct fluid  
868 equally well.

869 A similar argument can be applied to analysis of land topography and surface water flow.  
870 The “high resistance” (in principle, but not necessarily), localized small ‘humps of roughness  
871 elements’, and surface tension effects – analogous to the low  $K$  cells given in the previous  
872 paragraph – can be overcome, to allow development of preferential pathways that do not  
873 always follow the path of steepest descent in terms of surface topography. There are thus  
874 small bypassing effects. Moreover, there is flow/transport from land surface into the  
875 subsurface (e.g., hyporheic zone), which also “bypasses” localized small “humps” in the land  
876 surface and allows fluid connection/communication further downstream (along a pathway).

877 As a consequence, we argue that it is misleading to place undue focus on the high resistance  
878 (or surface “hump”) bottlenecks; rather, it should be recognized that entire “high K” or  
879 “potential” regions for flow are often unsampled or barely sampled by flowing water and  
880 chemicals, at least over moderate time scales.

881 To further expand on the link between spatial and temporal heterogeneity, we point out  
882 that the key is to think in space-time and complementary manifestations of heterogeneity of  
883 preferential flow. We already showed that a heterogeneous preferential flow pattern implies  
884 that chemical species leave the system at distinct locations, which implies a strong reduction  
885 in Shannon entropy, as shown in Sect. 2.4 for the example of Ederly et al. (2014). When  
886 observed at a fixed outlet, these heterogeneous flow patterns translate into signatures of the  
887 breakthrough curve. Again, this can be quantified through the corresponding deviations from  
888 a Fickian breakthrough curve, which is the maximum entropy travel time distribution,  
889 reflecting well-mixed, advective-dispersive transport (Tefry et al., 2003). The overall key  
890 messages of Sect. 3 are that (a) CTRW is consistent with the advection-dispersion equation  
891 and advances beyond it, particularly in terms of capturing dispersion and tailing effects, and  
892 (b) the power law exponent is related to porous media characteristics as well as the flow  
893 conditions, although this relation is not unique. Nevertheless, the opportunity arises to at least  
894 partly constrain spatial signatures of the subsurface from temporal ones with uncertainty. This  
895 non-uniqueness is another manifestation of the inherent equifinality problem, when reviewing  
896 model concepts in catchment science in Sect. 2.1.

897 In the next section, we adopt a temporal framework to introduce continuous time random  
898 (CTRW) theory, which is the basis of our proposed means to unify quantification of  
899 groundwater and surface water transport dynamics.

### 900 **3.3 Continuous Time Random Walks: Theory**

901 Preferential flow leads to non-Fickian (or “anomalous”) travel time distributions,  
902 characterised by rapid breakthrough and/or long tailing of chemical species through  
903 heterogeneous domains. The CTRW framework is well suited to deal with this in a manner  
904 that is consistent with microscale physics, and it steps beyond the advection-dispersion  
905 equation approach. This might also offer opportunities to understand SAS from a bottom up  
906 perspective, as age ranked storage relates to the integral of the travel time distribution across  
907 all ages.

908 Detailed descriptions of CTRW can be found in, e.g., Berkowitz et al. (2006, 2016). Here,  
909 we present only a brief outline of the essential elements. The CTRW framework is based on  
910 direct incorporation of the distribution of flow field fluctuations and thus of the fluctuations in  
911 concentrations of transported chemicals. As such, the CTRW is a time-nonlocal approach that  
912 can quantify chemical transport over a range of length (and time) scales, and address other  
913 processes such as chemical reactions.

914 From a microscale of view, “particles”, representing dissolved chemical species, are used  
915 to treat chemical transport; each particle undergoes spatiotemporal transitions – “transitions  
916 (or steps) in a random walk” – that encompass both displacement due to structural  
917 heterogeneity and the time taken to make each particle movement. Unlike other approaches,  
918 the formulation focuses on retaining the full distribution of transition times. Thus, CTRW  
919 defines a probability density function (PDF),  $\psi(\mathbf{s}, t)$ , of a random walk that couples the spatial



920 displacement  $\mathbf{s}$  and time  $t$  of the transition. As shown in Dentz et al. (2008), it is convenient  
 921 and generally applicable (but not obligatory) to use the decoupled form  $\psi(\mathbf{s}, t) = p(\mathbf{s})\psi(t)$ ,  
 922 where  $\psi(t)$  is the probability rate for a transition time  $t$  between sites, and  $p(\mathbf{s})$  is the  
 923 probability distribution of the length of the transitions. We stress here that the particle  
 924 *transition* time distribution represents the PDF of times for any given particle transition over  
 925 the distance  $\mathbf{s}$ , while the *travel* time distribution – also called a “first passage time  
 926 distribution” – discussed above and below is the PDF of arrival times (an “overall response”)  
 927 through a catchment, soil column, or aquifer at a measurement point or plane. A breakthrough  
 928 curve, representing the concentration of all particles arriving at a control/measurement point  
 929 (or plane) over time, can then be determined by calculating the average travel (first passage)  
 930 times of all particles exiting boundary of the flow domain. Thus, the *transition* time  
 931 distribution – however chosen – is the PDF underlying the resulting solution (which can be  
 932 characterized in terms of the breakthrough curve, as well as *travel* time, or first passage time,  
 933 distribution, as well as in terms of spatial profiles and moments) of the governing transport  
 934 equation; see Sect. 3.4 for further discussion. [Note: Regarding first passage time distributions  
 935 and breakthrough curves, a subtlety must be kept in mind, namely, that the breakthrough  
 936 curve is equal to the first passage time distribution if one measures it at an absorbing  
 937 boundary (“exiting the flow domain” could be represented by an absorbing boundary).  
 938 Otherwise, the flux-averaged concentration is obtained from the net flux across a boundary  
 939 (Simmons, 1982; or Appendix of Dentz et al., 2004). Nevertheless, the analytical expressions  
 940 for the first passage time distribution and flux concentration are equal under certain boundary  
 941 conditions.]

942 The defining transport equation is equivalent to a generalized master equation (GME),  
 943 which is essentially a mass balance equation in space and time. Using a Taylor expansion, the  
 944 GME can be transformed into the continuum version (ensemble-averaged system) of the  
 945 CTRW, in the form of an integro-partial differential equation:

$$946 \quad \frac{\partial c(\mathbf{s}, t)}{\partial t} = \int_0^t dt' M(t - t') [-\mathbf{v}_\psi \cdot \nabla \tilde{c}(\mathbf{s}, t') + \mathbf{D}_\psi : \nabla \nabla \tilde{c}(\mathbf{s}, t')] \quad (\text{Eq. 7})$$

948  
 949 for the normalized concentration  $c(\mathbf{s}, t)$ , where  $M$  is a memory function, the transport velocity  
 950  $\mathbf{v}_\psi$  and the generalized dispersion  $\mathbf{D}_\psi$  are defined in terms of the first and second moments of  
 951  $p(\mathbf{s})$ , and with the dyadic symbol  $:$  denoting a tensor product. In Laplace space, (1) becomes

$$952 \quad u\tilde{c}(\mathbf{s}, u) - c_o(\mathbf{s}) = -\tilde{M}(u)[\mathbf{v}_\psi \cdot \nabla \tilde{c}(\mathbf{s}, u) - \mathbf{D}_\psi : \nabla \tilde{c}(\mathbf{s}, u)] \quad (\text{Eq. 8})$$

954  
 955 where the memory function  $\tilde{M}(u) \equiv \bar{t}u\tilde{\psi}(u) / [1 - \tilde{\psi}(u)]$ ,  $\bar{t}$  is a characteristic time, and with  
 956  $\sim$  denoting Laplace space and  $u$  denoting the Laplace variable. Note that this continuum  
 957 formulation contains a nonlocal-in-time convolution, in terms of the memory function.

958 In contrast to the classical advection-dispersion equation (see Eq. (11), below), the  
 959 “transport velocity,”  $\mathbf{v}_\psi$  is in principle distinct from the “average fluid velocity,”  $\mathbf{v}$ . This is  
 960 because chemical transport is “clearly identifiable”, subject to diffusive and dispersive  
 961 mechanisms (recall the discussion following Fig. 6), so that the effective, overall transport  
 962 (i.e., a “characteristic” velocity) of chemical may be faster or slower than the average fluid

963 velocity. We point out, moreover, that residence times are a key characterisation, as they  
 964 generally differ for water and chemical species. To illustrate, it is sufficient to recognise that  
 965 the preferential flow paths themselves are generally stable when the overall hydraulic gradient  
 966 changes (unless dealing with significant changes or turbulent flow), so that the residence time  
 967 dictates the relative influence of diffusion and chemical movement into and out of less mobile  
 968 zones, which ultimately affects breakthrough curves (Berkowitz and Scher, 2009).

969 It is critical to recognize that the occurrence of “rare events” – even a small proportion of  
 970 chemical species migrating extremely slowly in some regions, and/or being repeatedly  
 971 trapped and released of slow regions over a series of spatial transitions – are sufficient to lead  
 972 to anomalous transport and extremely long “average” chemical transport times (Berkowitz et  
 973 al., 2016). Thus, it is important to differentiate between “average” (recall Sect. 3.1) and  
 974 “effective” transport of “most” particles. Indeed, we emphasise, too, that the effects of these  
 975 “rare events” are deeply significant: they do not simply average out, but rather propagate to  
 976 larger time and space scales.

977 With the decoupled form  $\psi(\mathbf{s}, t) = p(\mathbf{s})\psi(t)$ , the transition time distribution,  $\psi(t)$ , is thus at  
 978 heart of the CTRW framework, and its form determines the memory function; the role of  $p(\mathbf{s})$   
 979 on non-Fickian transport is relatively insignificant as long it has a compact (finite) range  
 980 (Dentz et al., 2008). As discussed in detail (e.g., Berkowitz et al., 2006, 2016), it is expedient  
 981 to define  $(t)$  as a truncated power law (TPL), which enables an evolution to Fickian  
 982 behaviour:

$$983 \quad \psi(t) = \frac{n}{t_1} \exp(-t/t_2) / (1 + t/t_1)^{1+\beta} \quad (\text{Eq. 9})$$

984 for  $0 < \beta < 2$ , with the normalization constant

$$985 \quad n \equiv (t_1/t_2)^{-\beta} \exp(-t_1/t_2) / \Gamma(-\beta, t_1/t_2) \quad (\text{Eq. 10})$$

986 and with  $\Gamma(-\beta, t_1/t_2)$  denoting the incomplete Gamma function (Abramowitz and Stegun,  
 987 1970). This functional form of  $\psi(t)$  has been particularly successful in interpreting a wide  
 988 range of laboratory and field observations, as well as numerical simulations. We chose the  
 989 characteristic time appearing in the memory function to be  $t_1$ , which represents the onset of  
 990 the power law region. The truncated power law form of  $\psi(t)$  behaves as a power law  
 991 proportional to  $(t/t_1)^{-1-\beta}$  for transition times in the range  $t_1 < t < t_2$ ;  $\psi(t)$  decreases  
 992 exponentially for transition times  $t > t_2$ . Thus, the TPL enables quantification of non-Fickian  
 993 transport, with a finite (sufficiently small)  $t_2$ , it facilitates (where appropriate) a longer-time,  
 994 smooth evolution to Fickian transport. We note, too, that the CTRW framework also  
 995 simplifies (e.g., Berkowitz et al., 2006, 2016) to specialized subsets of non-Fickian transport  
 996 behaviour embodied within, e.g., multirate mass transfer (Haggerty and Gorelick, 1995) and  
 997 fractional derivative (Zhang et al., 2009) formulations.

998 It is important to recognize, too, that specification of a pure exponential form for  $\psi(t)$ ,  
 999 namely  $\psi(t) = \lambda \exp(-\lambda t)$ , with mean  $1/\lambda$ , and/or choice of  $\beta > 2$ , reduces the CTRW transport  
 1000 Eq. (7) to the classical advection-dispersion equation, given in a general form as  
 1001

1006 
$$\frac{\partial c(\mathbf{s}, t)}{\partial t} = -\mathbf{v}(\mathbf{s}) \cdot \nabla c(\mathbf{s}, t) + \nabla \cdot [\mathbf{D}(\mathbf{s}) \nabla c(\mathbf{s}, t)]$$
 (Eq. 11)

1007

1008 where  $\mathbf{v}(\mathbf{s})$  is the velocity field and  $\mathbf{D}(\mathbf{s})$  is the dispersion tensor.

1009 It is thus clear that the power law exponent  $\beta$  in  $\psi(t)$  characterises the local disorder of the  
 1010 system and the degree of non-Fickian transport as an integral, temporal fingerprint in the  
 1011 breakthrough curves. This reflects the effect of a strongly localised preferential movement of  
 1012 chemical species on travel times (recall Fig. 4), caused by the pattern of local driving  
 1013 gradients and hydraulic conductivity. Because the particle movement is clearly organised in  
 1014 *space*, we suggest that this might be seen as self-organisation: local disorder is manifested in  
 1015 deviation from advective-dispersive transport, which leads to *non-local*, organised dynamic  
 1016 behaviour in *time* at the system scale. This implies that the CTRW framework provides a  
 1017 means to quantify the integral, temporal fingerprint of spatially organised preferential flow  
 1018 through the power law exponent  $\beta$  and the related distance from a Gaussian travel time  
 1019 distribution.

1020 The CTRW transport equation, in partial differential equation form, can be solved in  
 1021 Laplace space (Cortis and Berkowitz, 2005) as well as in real space (Ben-Zvi et al., 2019).  
 1022 One can also solve the transport equation by implementing various particle-tracking  
 1023 formulations. This was done, for example, to obtain the fits to the long-tailed breakthrough  
 1024 curve displayed in Fig. 6. Particle tracking (PT) approaches offer an efficient numerical tool  
 1025 to treat a variety of chemical transport scenarios (for both conservative and reactive chemical  
 1026 species). They are particularly well-suited to accounting for pore-scale to column-scale  
 1027 dynamics. “Particles” (representing chemical mass) advance by sampling transitions in space  
 1028 and time from the associated CTRW distributions. We emphasize that this PT approach can  
 1029 be employed to treat both advection-dispersion equation (Fickian, normal transport) and  
 1030 CTRW (non-Fickian, anomalous transport) formulations, via appropriate choice of  
 1031 (exponential or power law, respectively)  $\psi(t)$ .

1032 The efficacy and relevance of the CTRW framework has been demonstrated extensively  
 1033 for subsurface chemical transport (Berkowitz et al., 2006, 2016; Berkowitz and Scher, 2009;  
 1034 and references therein), from pore to aquifer scales, on the basis of extensive numerical  
 1035 simulations, laboratory experiments and field measurements. The formulation for chemical  
 1036 transport is general and robust over length scales ranging from pore to field, for different flow  
 1037 rates within the same domain, for chemically-reactive species, and even for time-dependent  
 1038 velocity fields (Nissan et al., 2017).

1039 To conclude this section, and bridge to discussion that follows in the next section, we  
 1040 point out here that, the *curved power law* form can in some cases be a useful representation  
 1041 rather than the truncated power law (TPL), Eq. (9), as shown by Nissan and Berkowitz  
 1042 (2019). In this case, we write  $\psi(t)$  as a curved power law function (Chabrier, 2003)

1043

1044 
$$\psi(t) = C_1 t^{-1-\beta} \exp(-t^*/t)$$
 (Eq. 12)

1045

1046 where  $C_1 \equiv (t^*)^\beta / \Gamma(\beta)$ , is the normalization constant of the probability density function and  $\Gamma$   
 1047 is the Gamma function. Here,  $t^*$  (a characteristic time) controls the exponential increase, while  
 1048  $\beta$  accounts for the power law region. It is important to note that this curved power law is an

1049 *inverse gamma distribution*, with shape parameter  $\beta$  and scale (or rate) parameter  $t^*$ . Note that  
1050 unlike the TPL in Eq. (9), notwithstanding the exponential term in Eq. (12), there is no cut-off  
1051 time that enables a transition to Fickian transport. These perspectives will be discussed in  
1052 detail in Sect. 3.4.

### 1053 **3.4 Continuous Time Random Walks: Application to surface water systems**

1054 In the context of our discussion in Sects. 2 and 3.1, recognizing that dynamics of chemical  
1055 transport in surface water and groundwater systems are at least phenomenologically and  
1056 functionally/dynamically similar over enormous spatial and temporal scales, we argue there  
1057 that simulations and analysis using the CTRW framework are meaningful and applicable also  
1058 to quantifying the (anomalous) dynamics of chemical transport in surface water systems. In  
1059 both surface water and groundwater systems, there is always “unresolved heterogeneity” (e.g.,  
1060 hydraulic conductivity, structure) at all scales. Fluid and chemical inputs range from being  
1061 reasonably well-defined to unknown (e.g., in terms of location and extent of a subsurface  
1062 contamination leak, areal extent and space-time heterogeneities of rainfall and related stable  
1063 isotope concentrations), while outputs may also be reasonably well-defined to unknown (e.g.,  
1064 arrival times of a chemical species to a monitoring point downstream, such as a stream gauge,  
1065 near surface spring or tile drain outlet). As a consequence, efforts to delineate preferential  
1066 flow paths and quantify chemical transport must be “adjusted” (or “be appropriate”) to the  
1067 level of knowledge and spatial/temporal resolution.

1068 More specifically, we note that the preferential pathways shown in Fig. 4b,c are  
1069 (phenomenologically, at least) similar to those of surface water systems shown in Fig. 1,  
1070 while the (temporal) breakthrough curves in Fig. 5 are similar to those determined at stream  
1071 gauges and tile drain outlets. Clearly, in surface water systems, and throughout small,  
1072 intermediate and large scales, there are stable regions of “water pockets” (less mobile water)  
1073 that can be distinguished by strongly varying chemical (ionic, isotopic) compositions. The  
1074 presence of tributaries leading to rivers in catchments demonstrates clear channelling effects  
1075 and the establishment of preferential pathways (Sect. 2).

1076 Before discussing chemical transport and considering CTRW applications in the context  
1077 of surface water systems, we emphasise – as described early in Sect. 3.3 – the  
1078 interrelationship between transition time distributions, travel time distributions, and  
1079 breakthrough curves. The *transition* time distribution, as used particularly in the context of  
1080 particle tracking and random walk model formulations, is the underlying (“building block”)   
1081 characterization of chemical movement in the domain. In other words, the *transition* time  
1082 distribution controls the nature of the overall transport. The *travel* time distribution is  
1083 obtained as the normalized histogram of the travel times (which can be based on the *transition*  
1084 time distribution) over all flow paths, or in other words, the travel time is the sum of the  
1085 individual transition times and the distribution is obtained by sampling over all travel times.  
1086 [Note: If one integrates the travel time distribution over all particles entering the system (in  
1087 space and in time), for a step input, one obtains the cumulative breakthrough curve ( $c$  vs.  $t$ ).  
1088 The relation between flux concentrations, pulse inputs, and breakthrough curves, relative to  
1089 the first passage time distribution for a homogeneous medium, is discussed in Section 3.1 of  
1090 Dentz and Berkowitz, 2003.)]

1091 In the context of these three types of quantification of chemical movement, and in light of  
1092 consideration of Eqs. (3) and (6) and the analysis to follow below, we stress the fundamental  
1093 importance of the underlying transition time distribution in quantifying chemical transport  
1094 through an aquifer or catchment. Common formulations of the governing transport equation,  
1095 particularly the advection-dispersion equation and many variants thereof, do not include an  
1096 explicit accounting of the transition or travel time distributions. However, as seen from the  
1097 discussion of Eq. (11), an underlying exponential transition time distribution in the CTRW  
1098 transport equation leads to the advection-dispersion equation with a Gaussian breakthrough  
1099 curve. In sharp contrast, in the case of a power law transition time distribution that scales as  
1100 scales as  $t^{-1-\beta}$ , such as given in Eqs. (9) and (12), the resulting breakthrough curve for a  
1101 point/pulse input also scales as  $t^{-1-\beta}$ , as a direct consequence of the generalized central limit  
1102 theorem (e.g., Dentz and Berkowitz, 2003, Eqs. (73) and (82)). For a step input, the scaling is  
1103  $t^{-\beta}$ , because it can be obtained from the point by integration in time.

1104 CTRW has also been applied in some partially saturated soil-water systems, which further  
1105 strengthens the connection of CTRW to surface water systems; as discussed in Sects. 2 and  
1106 3.1 (Figs. 4a,b), surface water flow and associated chemical transport are not purely overland  
1107 processes, but involve coupled interactions with the partially saturated (vadose) zone (Sect.  
1108 2.3) and groundwater zone (Sect. 2.4).

1109 Indeed, CTRW methods (and subsets) have already been applied in some sense, at least  
1110 qualitatively, to interpret anomalous transport in various surface water system scenarios. For  
1111 example, Boano et al. (2007) used CTRW to quantify chemical transport in a stream,  
1112 accounting for fluid-chemical interactions with the underlying sediment (i.e., the hyporheic  
1113 zone). Other studies have recorded power law and related multirate rate mass transfer  
1114 dynamics for chemical transport in stream and catchment systems (e.g., Haggerty et al., 2002;  
1115 Gooseff et al., 2003). These authors note, in particular, that the hyporheic zone exhibits an  
1116 enormous range of time scales over which chemical exchange can occur, with significant  
1117 amounts of chemical species being retained over extremely long times.

1118 However, while full application of CTRW to catchment-scale surface water systems has  
1119 not been reported to date, there are additional strong indications that it is applicable. We point  
1120 out two key aspects to support this claim, from the catchment hydrology literature. As  
1121 discussed in Sect. 2.2.3, previous studies used a gamma distribution to parameterize travel  
1122 time distributions (e.g., Hrachowitz et al., 2010), while more recent studies use a single or  
1123 several gamma distributions to characterise StorAgeSelection functions of stream flow and  
1124 evaporation. The gamma distribution, used particularly in connection with arrival times of  
1125 stable isotopes at a catchment outlet (= river outlet, measurement control plane) – i.e., as a  
1126 *travel* time distribution – has been applied to describe the superposition of different functions  
1127 to account for time dependence (e.g., Hrachowitz et al., 2010). Related directly to this point,  
1128 too, are unit hydrograph analyses that were used in the past to describe runoff concentration  
1129 and flood routing, through a Nash Cascade, which is essentially a gamma distribution, as  
1130 discussed also in Sect. 2.2.3. We now focus on this aspect in detail.

1131 The gamma distribution is given by

1132

1133

1134

$$P(t) = C_2 t^{-1+\beta} \exp(-t t^*), \quad (\text{Eq. 13})$$

1135

1136 where  $C_2 \equiv (t^*)^\beta / \Gamma(\beta)$ , or, equivalently (and for comparison to Eq. (12)),

1137

$$1138 \quad P(t) = C_3 t^{-1+\beta} \exp(-t/t^*), \quad (\text{Eq. 14})$$

1139

1140 where  $C_3 \equiv 1/[(t^*)^\beta \Gamma(\beta)]$ . The gamma distribution describes processes for which the waiting  
1141 times between Poisson distributed events are important.

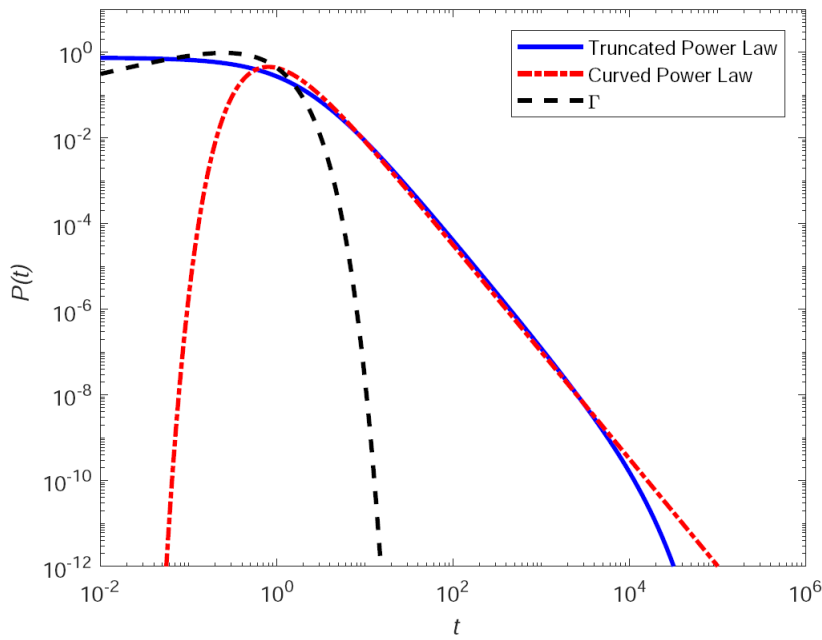
1142 In light of Sect. 2, and the discussion of transition and travel time distributions in Sect. 3.3  
1143 and above, we consider what underlying *transition* time distribution leads to a gamma  
1144 distributed *travel* time. Given that a sum of gamma distributed random variables can also be  
1145 gamma distributed, the choice of a gamma distribution for both *transition* and *travel* time  
1146 distributions is convenient. -et al., 2017).

1147 Indeed, in terms of transition time distributions, let us compare the gamma distribution in  
1148 the form of Eq. (14) to the inverse gamma distribution as shown in Eq. (12). Aside from the  
1149 normalisation coefficients, the inverse gamma and gamma distributions shown in Eqs. (12)  
1150 and (14) differ in two fundamental ways – the power law (exponent of  $t$ ) terms,  $t^{-1-\beta}$  vs.  $t^{-1+\beta}$   
1151 and the exponential terms,  $\exp(-t^*/t)$  vs.  $\exp(-t/t^*)$ , respectively. We stress again, as explained  
1152 in Sect. 3.2, that the *inverse* gamma distribution is a power law distribution (without an  
1153 exponential cut-off time to allow transition to Fickian transport), and thus one form of  
1154 transition time distribution  $\psi(t)$  in the CTRW formulation.

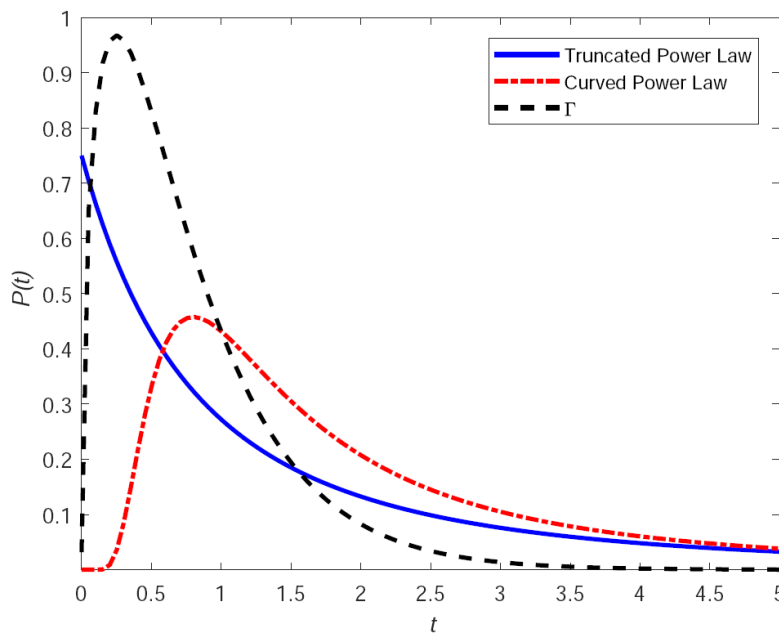
1155 We plot in Fig. 7a the truncated power law, curved power law (inverse gamma) and  
1156 gamma (*transition* time) distributions,  $P(t)$ , for the specific parameters  $\beta = 1.5$ ,  $t_1 = 1$ ,  $t_2 = 10^3$ ,  
1157  $t^* = t_1$ . We plot in log-log scale to emphasize the long-time portion of the transition time  
1158 distribution. Figure 7b shows the same curves plotted on a linear scale, to contrast the fact that  
1159 linear plots (noting the short time scale on the  $x$ -axis) do not illustrate the long-time  
1160 contributions, which can have a critical effect on the overall transport behaviour. Clearly,  
1161 from Fig. 7b, the gamma distribution has does not include the possibility of long times; it has  
1162 an exponential cut-off to Gaussian behaviour at times larger than  $t^*$ , as the exponential term  
1163 dominates the power law term when  $t \gg t^*$ . However, note that the power law is  $t^{-1+\beta}$  rather  
1164 than  $t^{-1-\beta}$ . The inverse gamma distribution, on the other hand, does not display an exponential  
1165 cut-off, but has the same  $t^{-1-\beta}$  power law scaling as the TPL.

1166 We thus conclude (recall also the conceptual picture and discussion in Sect. 3.1) that  
1167 although there is no universally “right” or “wrong” choice, the gamma (*transition* time)  
1168 distribution does not generally appear as a suitable “candidate” to quantify chemical transport  
1169 in surface water systems, notwithstanding its empirical use in the literature. We suggest that  
1170 the CTRW framework (Sect. 3.3) rests on a more physically justified conceptual picture and  
1171 corresponding, coherent and robust mathematical formulation; other such frameworks and  
1172 transition time distributions can of course also be considered, if justified physically. The  
1173 choice of a truncated power law or inverse gamma (*transition* time) distribution is largely a  
1174 function of scale. The inverse gamma distribution may better suit pore-scale (microscale)  
1175 domains, where the peak of the function is important, and where ergodicity is not relevant (the  
1176 cut-off is not needed). Using the truncated power law is “more” general, and better suits a  
1177 variety of larger scale problems.

1178



1179 (a)



1180 (b)

1181 **Figure 7** Truncated power law, curved power law (inverse gamma distribution) and gamma  
 1182 distribution, for the specific parameters:  $\beta = 1.5$ ,  $t_1 = 1$ ,  $t_2 = 10^3$ ,  $t^* = t_1$ . **(a)** Log-log scale to  
 1183 emphasise the long-time tailing behaviour. **(b)** Linear scale.

1184

1185 We now consider a specific example that demonstrates the relevance and applicability of  
 1186 the CTRW framework for chemical transport in surface water systems, keeping the above  
 1187 arguments in mind. Referring to the 2D case shown in Fig. 6a, we consider the effective  
 1188 (travel time distribution) response,  $h(t)$ , to a rainfall pulse containing a chemical species over  
 1189 the entire area of a catchment. Every point over this area may be considered a source of chemical  
 1190 species (“tracer”). A stream running through the catchment acts as a line sink (collector) for  
 1191 the tracer. This catchment picture can be idealised as two rectangles straddling this stream

1192 sink (Fig. 6a). Measurements of tracer arrivals at a control point downstream of this stream  
 1193 (known as an “absorbing boundary”) yield a tracer arrival “counting rate” that is a  
 1194 breakthrough curve.

1195 The first-passage time distribution  $F(\mathbf{l}_s, t)$  defines the travel time distribution from a  
 1196 (pulse) source at the origin  $\mathbf{l}$  to the point  $\mathbf{l}_s$ . Then the chemical tracer/species concentration at  
 1197 position  $\mathbf{l}_s$  and time  $t$ ,  $c_s(\mathbf{l}_s, t)$  is given by

$$1198 \quad c_s(\mathbf{l}_s, t) = \int_0^\infty \sum_{\mathbf{l} \in \Omega} F(\mathbf{l}_s - \mathbf{l}, t') c_R(\mathbf{l}, t - t') dt' \quad (\text{Eq. 15})$$

1200 where  $c_R(\mathbf{l}, t)$  is the chemical input from rainfall at a position  $\mathbf{l}$  in a catchment of area  $\Omega$ .  
 1201 Referring then to Fig. 6a, because we sample chemical arrivals downstream, we can consider  
 1202 the sampling position as an “instantaneous” integration of all chemical species/tracer arrivals  
 1203 from the catchment pathways along the entire length of the stream. Travel time within the  
 1204 stream can generally be assumed negligible, relative to the catchment travel times, as stream  
 1205 velocities are generally much faster than combined overland/subsurface flows. We thus  
 1206 determine the total chemical flux into the stream by integrating over all chemical inputs in the  
 1207 catchment that reach the stream; this defines overall first-passage time distributions at the  
 1208 downstream measurement point. Assuming that all of the sampling positions in  $\mathbf{l}_s$  are small  
 1209 regions compared to  $\Omega$ , then  $c_s(\mathbf{l}_s, t) \approx c_s$ . For uniform rainfall distribution over  $\Omega$ , we have  
 1210  $c_R(\mathbf{l}, t) \approx c_R(t)$ , and we can hence define for the effective, overall response (travel time  
 1211 distribution)

$$1212 \quad h(t) \equiv \sum_{\mathbf{l} \in \Omega} F(\mathbf{l}, t) \quad (\text{Eq. 16})$$

1213  
 1214 Long-term measurements of chloride tracer concentrations  $c_R(t)$  in the rainfall over a  
 1215 catchment area in Plynlimon, Wales, were compared to the time series of the chloride tracer  
 1216 concentration  $c_s(t)$  in the catchment Hafren stream (Kirchner et al., 2000). These authors  
 1217 related the input and output concentrations through the convolution integral

$$1218 \quad c_s(t) = \int_0^\infty h(t') c_R(t - t') dt' \quad (\text{Eq. 17})$$

1220  
 1221 Using a spectral analysis, Kirchner et al. (2000) concluded that overall chloride transport in  
 1222 the catchment scaled as  $h(t) \sim t^{-m}$ , with  $m \approx 0.5$ , over a time period from 0.01 to 10 years.  
 1223 They reported similar scaling in North American and Scandinavian field sites with  $m \approx 0.4$ –  
 1224 0.65.

1225  
 1226 Kirchner et al. (2000) continued their analysis by noting (i) that an exponential travel time  
 1227 distribution (which is implicit in the advection-dispersion equation; see discussion above Eq.  
 1228 (11)) does not match the data, and (ii) that conceptualization of the entire catchment as a  
 1229 single flow path, and use of the advection-dispersion equation to describe travel times, do not  
 1230 correctly match even the basic character of the chloride concentration arrivals. The authors  
 1231 concluded that catchment travel time distributions should be quantified as an approximate  
 1232 power law distribution, to correctly account for long-time chemical retention and release in  
 1233 catchments, and defined  $h(t)$  as a gamma distribution (recall Eq. (14)). It should be recognised  
 1234



1235 that the choice of a gamma distribution is empirical, and other functions can generate similar  
 1236 behaviours in the spectral (Laplace or Fourier) domain. Significantly, the slope identified by  
 1237 Kirchner et al. (2000) reflects high frequencies, i.e., short time scales; several decades of  
 1238 tracer data to validate the power spectrum at low frequencies were not available.

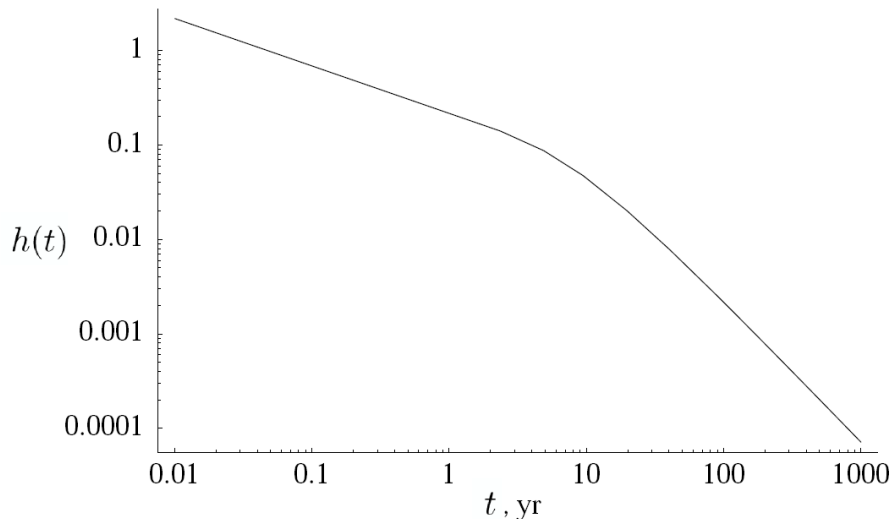
1239 Scher et al. (2002) reanalysed this catchment system behaviour with the CTRW  
 1240 framework, arguing that subsurface flow and transport are dominant factors controlling the  
 1241 overall chemical species arrival to the stream outlet measurement point. Based on Eqs. (15)  
 1242 and (16), they first (re)examined the solution of the one-dimensional advection-dispersion  
 1243 equation; they confirmed that the temporal dependence of  $h(t)$  does not represent the field  
 1244 measurements (similar to Kirchner et al., 2000). Significantly, though, they employed a pure  
 1245 power law form of the transition time distribution,  $\psi(t) \sim t^{-1-\beta}$ , and developed Eqs. (15) and  
 1246 (16) – based on the seminal analysis of Scher and Montroll (1975) – to obtain

$$1247 \quad h(t) \sim \begin{cases} t^{-1+\beta}, & t < t^* \\ t^{-1-\beta}, & t > t^* \end{cases} \quad \text{for } 0 < \beta < 1. \quad (\text{Eq. 18})$$

1249 The turnover time  $t^*$  between these two slopes arises naturally as an outcome of chemical  
 1250 transport in the system embodied in Eq. (16). The smaller times represent chemical inputs  
 1251 following along fastest flow paths to the sampling point; for  $t > t^*$ , all chemical inputs over  
 1252 the entire catchment area are contributing particles to the sampling point, as accounted for in  
 1253 Eq. (17). In this latter case, the power law represents the overall particle movement in the  
 1254 domain, but especially the effects of the slow particles (longer transition times and influence  
 1255 of less mobile zones) and the longer travel distances.

1257 In the context of the Hafren stream system, the turnover time  $t^*$  was estimated as about 10  
 1258 years (Scher et al., 2002), in agreement with findings and measurement range of Kirchner et  
 1259 al. (2000), with  $\beta = 0.5$ . Figure 8 shows a representative plot of Eq. (18) for this system. As  
 1260 noted in Scher et al. (2002), it remains to analyse measurements to confirm the turnover to the  
 1261 longer-time  $t^{-1-\beta}$  scaling behaviour, which is indicative of extremely long retention times.  
 1262 Note that high-resolution measurements of low concentration levels in water are generally  
 1263 required to analyse these longer-time tails. The key recognition here is that while the effective  
 1264 catchment response *may potentially*, initially (i.e., at relatively short times), be represented by  
 1265 a type of gamma distribution (i.e., a power law  $\sim t^{-1+\beta}$ , ignoring the exponential cut-off) at  
 1266 sufficiently small times (<10 years in the case of the Hafren catchment) – and this is  
 1267 embodied in the CTRW framework as seen in Eq. (18) – full (CTRW framework) power law  
 1268 behaviour (i.e.,  $\sim t^{-1-\beta}$ ) over longer times should also be incorporated to describe expected  
 1269 long-term catchment retention behaviour. An evolution to Fickian transport, via an  
 1270 exponential cut-off at very long times, can also be included (if relevant). To conclude, while  
 1271 direct, quantitative application of CTRW to analysis of chemical transport at the catchment  
 1272 scale remains to be done, it appears – on the basis of the conceptual pictures, extensive  
 1273 application to subsurface systems and direct similarities to catchment systems, and the robust  
 1274 and general nature of the CTRW formulation – to be a highly promising avenue for future  
 1275 research.

1276



1277  
 1278 **Figure 8** A log-log plot of  $h(t)$  vs.  $t$  (after Scher et al., 2002; Copyright 2002, with permission  
 1279 from the American Geophysical Union).  
 1280

## 1281 4 CONCLUSIONS AND PERSPECTIVES

### 1282 4.1 Preferential flow and non-Gaussian travel times: The spatial and the 1283 temporal manifestation of organized complexity

1284  
 1285 Based on Sects. 2 and 3, we can state that (a) preferential flow and related non-Fickian  
 1286 transport is an omnipresent, unifying element between both water worlds, and (b) the CTRW  
 1287 framework can effectively quantify and predict non-Fickian transport of water and chemicals  
 1288 species in a manner that connects to and clearly steps beyond the advection-dispersion  
 1289 paradigm. In this section, we link these insights to our central proposition that preferential  
 1290 flow is a prime manifestation of how a local-scale heterogeneous flow process causes a  
 1291 macroscale organised flow pattern in *space*. The key is to acknowledge that organisation  
 1292 manifests also through organised dynamic behaviour in *time*, which occurs through non-  
 1293 Fickian travel time distributions of water and chemical species. Note that the degree of  
 1294 organisation in *space* manifests in the deviation of spatial patterns of system characteristics or  
 1295 fluid flow from the maximum entropy pattern. The latter corresponds, in the case that the  
 1296 mean value is known, to a uniform distribution of system characteristics and/or a uniform  
 1297 flow pattern. Along the same lines, we propose that the degree of organisation in dynamic  
 1298 behaviour in *time* manifests through the deviation of the breakthrough curve from the case of  
 1299 a well-mixed Gaussian system, which is quantified within the CTRW framework based on the  
 1300 power law exponent. A power law exponent  $\geq 2$  corresponds to well a mixed travel time  
 1301 distribution. The latter reflect a spatial concentration equal to a Gaussian, which maximises  
 1302 entropy when the *mean* and the *variance* are known (Trefry et al., 2003).

1303 In terms of how power law transition distributions are linked to the formation, evolution  
 1304 and function of preferential flow paths in surface water systems, and how and if they can be  
 1305 expected to improve representation thereof in models, we first emphasise that power law  
 1306 transition time distributions are linked to the *function* of preferential flow paths, but not to

1307 their formation and evolution. It is clear and well-known that preferential flow implies non-  
1308 Fickian residence times or travel distance. But what has not been recognized, though, is that  
1309 the fingerprint of preferential flow in the overall travel time distribution can be captured by a  
1310 (truncated) power law for the transition time distribution; and through the related exponent we  
1311 can quantify the deviation from the well-mixed Fickian case. As discussed in Sect. 2.4, the  
1312 findings of Edery et al. (2014) suggest a further connection between the characteristics of an  
1313 aquifer and the power law exponent in breakthrough curves. This implies that the fitted  
1314 parameters are a macroscale fingerprint of spatial media characteristics that determine the  
1315 temporal arrival of chemical species. While we do not expect that this relation is unique, it  
1316 does imply that “fitted” parameters have a physical meaning that can be used to constrain  
1317 characteristics of the domain (i.e., the hydrological landscape mentioned above) in a spatially  
1318 distributed model.

1319 We argue that this should also hold for other complex media characteristics that relate to  
1320 their spatial organization, such as the correlation length or topology of preferential flow paths.  
1321 We therefore suggest that these insights offer opportunities to relate signatures of spatial  
1322 organization in flow patterns to signatures of temporal organization in breakthrough curves.  
1323 For both perspectives, we can quantify organization using information entropy, as we showed  
1324 in Sect. 2.4. These arguments might also offer, ultimately, opportunities to test whether  
1325 hydrological systems and their preferential flow networks co-evolve towards more energy  
1326 efficient drainage, which can also be quantified (Kleidon et al. 2013; Zehe et al., 2019;  
1327 Savenije and Hrachowitz, 2017). We leave a more detailed reflection on this for future  
1328 studies.

## 1329 **4.2 Overall conclusions and perspectives**

1330 In an effort to integrate and unify conceptualisation and quantitative modelling of the two  
1331 “water worlds”– surface water and groundwater systems – we recognise preferential fluid  
1332 flows as a unifying element and consider them as a manifestation of self-organisation.  
1333 Preferential flows hinder perfect mixing within a system, due to a more “energy efficient” and  
1334 hence faster throughput of water, which affects residence times of water, matter and chemical  
1335 species in hydrological systems across all scales. While our main focus here is on the role of  
1336 preferential flow for residence times and chemical transport, we relate our proposed unifying  
1337 concept to role of preferential flow for energy conversions and energy dissipation associated  
1338 with flows of water and mass.

1339 Essentially, we have proposed that related conceptualisations on the role of heterogeneity  
1340 and preferential fluid flow for chemical species transport, and its quantitative characterisation,  
1341 can be unified in terms of a theory, based on the CTRW framework, that connects these two  
1342 water worlds in a dynamic framework. We emphasise the occurrence of power law  
1343 behaviours that characterise travel times of chemical species, and highlight the critical role  
1344 played by system heterogeneity and chemical species residence times, which are distinct from  
1345 travel times of water. In particular, we compare and contrast specific power law distributions,  
1346 and argue that the closely related inverse gamma and algebraic power law distributions are  
1347 more appropriate than the oft-used gamma distribution to quantify chemical species transport.

1348 Moreover, we identify deviations from well-mixed Gaussian transport as a manifestation  
1349 of self-organised dynamic behaviour in time, and the power law exponent as a suitable means

1350 to measure the strength of this deviation. Along a complementary line, we propose that self-  
1351 organisation in space is immanent primarily through strongly localised preferential flow  
1352 through rill and river networks at the land surface. We relate the degree of spatial organisation  
1353 to the deviation of the flow pattern from spatially homogeneous flow, which is a state of  
1354 maximum entropy. In this context, we reflect on the ongoing controversial discussion  
1355 regarding whether or not self-organisation in open hydrological systems leads to evolution to  
1356 a more energy efficient or even thermodynamic optimal system configuration. Finally, we  
1357 propose that our concept of temporally organised travel times can help to test the possible  
1358 emergence of thermodynamic optimality. Complementary to this idea, we suggest that an  
1359 energetic perspective of chemical species transport may help to explain the organisation of  
1360 travel paths (Fig. 4), in the sense that contrary to common assumptions, preferential pathways  
1361 often include “bottlenecks” of low hydraulic conductivity. A testable option could be that  
1362 chemical species travel along the path of maximum power, with power being defined in this  
1363 case as flow of chemical energy (rather than flow of kinetic energy) through the system.

1364 Overall, we conclude that self-organisation arises equally in surface water and  
1365 groundwater systems, as local heterogeneity and disorder in fluid flow and chemical transport  
1366 processes lead to ordered behaviour at the macroscale. Naturally, the surface water  
1367 community has developed a strong emphasis on the *localised spatial fingerprints*, because  
1368 rills and rivers are clearly visible on land (Fig. 1), while the groundwater community has  
1369 focused more naturally on *non-local temporal fingerprints*, as the flow paths are largely  
1370 unobservable. But these are just two sides of the same conceptual picture of organised  
1371 complexity (Dooge, 1986).

1372

1373 **Competing interests.** The authors declare that they have no conflict of interest.

1374

1375 **Acknowledgements.** The authors thank Markus Hrachowitz, Nicolas Rodriguez, Matthias  
1376 Sprenger, and an anonymous referee for particularly constructive reviews of this work. B.B.  
1377 gratefully acknowledges the support of research grants from the Israel Water Authority (Grant  
1378 No. 45015199895) and the Israel Science Foundation (Grant No. 485/16); he thanks Harvey  
1379 Scher for in-depth discussions. B.B. holds the Sam Zuckerberg Professorial Chair in  
1380 Hydrology. E.Z. gratefully acknowledges intellectual support by the "Catchments as  
1381 Organized Systems" (CAOS) research unit and funding of the German Research Foundation,  
1382 DFG, (FOR 1598, ZE 533/11-1, ZE 533/12-1).

1383

## 1384 5 REFERENCES

- 1385 Abramowitz, M. and Stegun, I.: Handbook of Mathematical Functions, Dover, Mineola, N.Y.,  
1386 1970.
- 1387 Angermann, L., Jackisch, C., Allroggen, N., Sprenger, M., Zehe, E., Tronicke, J., Weiler, M.,  
1388 and Blume, T.: Form and function in hillslope hydrology: Characterization of subsurface  
1389 flow based on response observations, Hydrology And Earth System Sciences, 21, 3727-  
1390 3748, doi:10.5194/hess-21-3727-2017, 2017.

1391 Aronofsky, J. S. and Heller, J. P.: A diffusion model to explain mixing of flowing miscible  
1392 fluids in porous media, *Trans. Am. Inst. Min. Metall. Pet. Eng.*, 210, 345-349, 1957.

1393 Bardossy, A.: Copula-based geostatistical models for groundwater quality parameters, *Water*  
1394 *Resour. Res.*, 42, W11416, doi:10.1029/2005wr004754, 2006.

1395 Bardossy, A.: Calibration of hydrological model parameters for ungauged catchments,  
1396 *Hydrol. Earth Syst. Sci.*, 11, 703-710, doi:10.5194/hess-11-703-2007, 2007.

1397 Bardossy, A. and Singh, S. K.: Robust estimation of hydrological model parameters, *Hydrol.*  
1398 *Earth Syst. Sci.*, 12, 1273-1283, doi:10.5194/hess-12-1273-2008, 2008.

1399 Bejan, A., Lorente, S., and Lee, J.: Unifying constructal theory of tree roots, canopies and  
1400 forests, *J. Theor. Biol.*, 254, 529-540, doi:10.1016/j.jtbi.2008.06.026, 2008.

1401 Benettin, P., Volkmann, T. H. M., von Freyberg, J., Frentress, J., Penna, D., Dawson, T. E.,  
1402 and Kirchner, J.: Effects of climatic seasonality on the isotopic composition of evaporating  
1403 soil waters, *Hydrol. Earth Syst. Sci.*, 22, 2881-2890, doi:10.5194/hess-22-2881-2018,  
1404 2018.

1405 Ben-Zvi, R., Jiang, S., Scher, H., and Berkowitz, B.: Finite-Element Method solution of non-  
1406 Fickian transport in porous media: The CTRW-FEM package, *Groundwater*, 57, 479-484,  
1407 doi:10.1111/gwat.12813, 2019.

1408 Berkowitz, B. and Scher, H.: Exploring the nature of non-Fickian transport in laboratory  
1409 experiments, *Adv. Water Resour.*, 32, 750-755, doi:10.1016/j.advwatres.2008.05.004,  
1410 2009.

1411 Berkowitz, B., Cortis, A., Dentz, M., and Scher, H.: Modeling non-Fickian transport in  
1412 geological formations as a continuous time random walk, *Rev. Geophys.*, 44, RG2003,  
1413 doi:10.1029/2005RG000178, 2006.

1414 Berkowitz, B., Dror, I., Hansen, S. K., and Scher, H.: Measurements and models of reactive  
1415 transport in geological media, *Rev. Geophys.*, 54, 930-986, doi:10.1002/2016RG000524,  
1416 2016.

1417 Beven, K.: Changing ideas in hydrology - the case of physically-based models, *J. Hydrol.*,  
1418 105, 157-172, doi:10.1016/0022-1694(89)90101-7, 1989.

1419 Beven, J. K. and Binley, A.: The future of distributed models: Model calibration and  
1420 uncertainty prediction, *Hydrol. Proc.*, 6, 265-277, doi:10.1002/hyp.3360060305, 1992.

1421 Beven, K. and Germann, K.: Macropores and water flow in soils, *Water Resour. Res.*, 18,  
1422 1311-1325, doi:10.1029/WR018i005p01311, 1982.

1423 Beven, K. and Germann, P.: Macropores and water flow in soils revisited, *Water Resour.*  
1424 *Res.*, 49, 3071-3092, doi:10.1002/wrcr.20156, 2013.

1425 Bianchi, M., Zheng, C., Wilson, C., Tick, G. R., Liu, G., and Gorelick, S. M.: Spatial  
1426 connectivity in a highly heterogeneous aquifer: From cores to preferential flow paths,  
1427 *Water Resour. Res.*, 47, W05524, doi:10.1029/2009WR008966, 2011.

1428 Binet, F., Kersante, A., Munier-Lamy, C., Le Bayon, R. C., Belgly, M. J., and Shipitalo, M. J.:  
1429 Lumbricid macrofauna alter atrazine mineralization and sorption in a silt loam soil, *Soil*  
1430 *Biol. Biochem.*, 38, 1255-1263, doi:10.1016/j.soilbio.2005.09.018, 2006.

1431 Bishop, J. M., Callaghan, M. V., Cey, E. E., and Bentley, L. R.: Measurement and simulation  
1432 of subsurface tracer migration to tile drains in low permeability, macroporous soil, *Water*  
1433 *Resour. Res.*, 51(6), 3956-3981, doi:10.1002/2014WR016310, 2015.

- 1434 Blume, T., Zehe, E., and Bronstert, A.: Investigation of runoff generation in a pristine, poorly  
 1435 gauged catchment in the Chilean Andes II: Qualitative and quantitative use of tracers at  
 1436 three spatial scales, *Hydrol. Proc.*, 22, 3676-3688, doi:10.1002/hyp.6970, 2008.
- 1437 Blume, T., Zehe, E., and Bronstert, A.: Use of soil moisture dynamics and patterns at different  
 1438 spatio-temporal scales for the investigation of subsurface flow processes, *Hydrol. Earth  
 1439 Syst. Sci.*, 13, 1215-1233, doi:10.5194/hess-13-1215-2009, 2009.
- 1440 Boano, F., Packman, A.I., Cortis, A., Revelli, R., and Ridolfi, L.: A continuous time random  
 1441 walk approach to the stream transport of solutes, *Water Resour. Res.*, 43, W10425,  
 1442 doi:10.1029/2007WR006062, 2007.
- 1443 Bodin, J.: From analytical solutions of solute transport equations to multidimensional time-  
 1444 domain random walk (TDRW) algorithms, *Water Resour. Res.*, 51, 1860-1871,  
 1445 doi:10.1002/2014WR015910, 2015.
- 1446 Bolduan, R. and Zehe, E.: Degradation of isoproturon in earthworm macropores and subsoil  
 1447 matrix - a field study, *J. Plant Nutrition Soil Sci.*, 169, 87-94, doi:10.1002/jpin.200521754,  
 1448 2006.
- 1449 Bonell, M., Pearce, A. J., and Stewart, M. K.: The identification of runoff-production  
 1450 mechanisms using environmental isotopes in a tussock grassland catchment, eastern Otago,  
 1451 New Zealand, *Hydrol. Proc.*, 4, 15-34, doi:10.1002/hyp.3360040103, 1990.
- 1452 Botter G., Bertuzzo E., and Rinaldo A.: Transport in the hydrologic response: Travel time  
 1453 distributions, soil moisture dynamics, and the old water paradox, *Water Resour. Res.*,  
 1454 46(3), W03514, doi:10.1029/2009WR008371, 2010.
- 1455 Botter G., Bertuzzo E., and Rinaldo A.: Catchment residence and travel time distributions:  
 1456 The master equation, *Geophys. Res. Lett.*, 38(11), L11403, doi:10.1029/2011GL047666,  
 1457 2011.
- 1458 Bundt, M., Widmer, F., Pesaro, M., Zeyer, J., and Blaser, P.: Preferential flow paths:  
 1459 Biological 'hot spots' in soils, *Soil Biol. Biochem.*, 33, 729-738, doi:10.1016/S0038-  
 1460 0717(00)00218-2, 2001.
- 1461 Camporese, M., Paniconi, C., Putti, M., and Orlandini, S.: Surface-subsurface flow modeling  
 1462 with path-based runoff routing, boundary condition-based coupling, and assimilation of  
 1463 multisource observation data, *Water Resour. Res.*, 46, W0251210,  
 1464 doi:1029/2008wr007536, 2010.
- 1465 Chabrier, G., Galactic stellar and substellar initial mass function, *Publ. Astron. Soc. Pac.* 115,  
 1466 763-795, doi:10.1086/376392, 2003.
- 1467 Collins, R., Jenkins, A., and Harrow, M. A.: The contribution of old and new water to a storm  
 1468 hydrograph determined by tracer addition to a whole catchment, *Hydrol. Processes*, 14,  
 1469 701-711. doi:10.1002/(SICI)1099-1085(200003)14:43.0.CO;2-2, 2000.
- 1470 Cortis A. and Berkowitz B.: Computing "anomalous" contaminant transport in porous media:  
 1471 The CTRW MATLAB toolbox, *Ground Water*, 43, 947-950, doi:10.1111/j.1745-  
 1472 6584.2005.00045.x, 2005.
- 1473 Davies, J. and Beven, K.: Comparison of a multiple interacting pathways model with a  
 1474 classical kinematic wave subsurface flow solution, *Hydrol. Sci. J.-J. Sci. Hydrol.*, 57, 203-  
 1475 216, doi:10.1080/02626667.2011.645476, 2012.

1476 Davies, J., Beven, K., Rodhe, A., Nyberg, L., and Bishop, K.: Integrated modeling of flow  
1477 and residence times at the catchment scale with multiple interacting pathways, *Water*  
1478 *Resour. Res.*, 49, 4738-4750, doi:10.1002/wrcr.20377, 2013.

1479 Dentz, M., and Berkowitz, B.: Transport behavior of a passive solute in continuous time  
1480 random walks and multirate mass transfer, *Water Resour. Res.*, 39, 1111,  
1481 doi:[10.1029/2001WR001163](https://doi.org/10.1029/2001WR001163), 2003.

1482 Dentz, M., Cortis, A., Scher, H., and Berkowitz, B.: Time behavior of solute transport in  
1483 heterogeneous media: Transition from anomalous to normal transport, *Adv. Water Resour.*,  
1484 27(2), 155-173, doi:10.1016/j.advwatres.2003.11.002, 2004.

1485 Dentz, M., Scher, H., Holder, D., and Berkowitz, B.: Transport behaviour of coupled  
1486 continuous-time random walks, *Phys. Rev. E*, 78, 41110,  
1487 doi:10.1103/PhysRevE.78.041110, 2008.

1488 Dooge, J. C. I.: Looking for hydrological laws, *Water Resour. Res.*, 22, 46S-58S,  
1489 doi:10.1029/WR022i09Sp0046S, 1986.

1490 Duan, Q. Y., Sorooshian, S., and Gupta, H.V.: Effective and efficient global optimization for  
1491 conceptual rainfall-runoff models, *Water Resour. Res.*, 28, 1015-1031,  
1492 doi:10.1029/91WR02985, 1992.

1493 Ebel, B. A., and Loague, K.: Physics-based hydrologic-response simulation: Seeing through  
1494 the fog of equifinality, *Hydrol. Process.*, 20(13), 2887-2900, doi:10.1002/hyp.6388, 2006.

1495 Edery, Y., Guadagnini, A., Scher, H., and Berkowitz, B.: Origins of anomalous transport in  
1496 disordered media: Structural and dynamic controls, *Water Resour. Res.*, 50, 1490-1505,  
1497 doi:10.1002/2013WR015111, 2014.

1498 Everett, M. E.; *Near-Surface Applied Geophysics*, Cambridge University Press, Cambridge,  
1499 2013.

1500 Ewen, J.: 'Samp' model for water and solute movement in unsaturated porous media involving  
1501 thermodynamic subsystems and moving packets 1. Theory, *J. Hydrol.*, 182, 175-194,  
1502 doi:10.1016/0022-1694(95)02925-7, 1996a.

1503 Ewen, J.: 'Samp' model for water and solute movement in unsaturated porous media involving  
1504 thermodynamic subsystems and moving packets 2. Design and application, *J. Hydrol.*, 182,  
1505 195-207, doi:10.1016/0022-1694(95)02926-5, 1996b.

1506 Faulkner, H.: Connectivity as a crucial determinant of badland morphology and evolution,  
1507 *Geomorphology*, 100, 91-103, doi:10.1016/j.geomorph.2007.04.039, 2008.

1508 Fenicia, F., Kavetski, D., and Savenije, H. H. G.: Elements of a flexible approach for  
1509 conceptual hydrological modeling: 1. Motivation and theoretical development, *Water*  
1510 *Resour. Res.*, 47, W11510, doi:10.1029/2010wr010174, 2011.

1511 Fenicia, F., Kavetski, D., Savenije, H. H. G., Clark, M. P., Schoups, G., Pfister, L., and Freer,  
1512 J.: Catchment properties, function, and conceptual model representation: Is there a  
1513 correspondence?, *Hydrol. Proc.*, 28, 2451-2467, doi:10.1002/hyp.9726, 2014.

1514 Fenicia, F., Savenije, H. H. G., Matgen, P., and Pfister, L.: A comparison of alternative  
1515 multiobjective calibration strategies for hydrological modelling. *Water Resour. Res.*, 43,  
1516 W03434, doi:10.1029/2006WR005098, 2007.

1517 Feyen, L., Vazquez, R., Christiaens, K., Sels, O., and Feyen, J.: Application of a distributed  
1518 physically-based hydrological model to a medium size catchment, *Hydrol. Earth Syst. Sci.*,  
1519 4, 47-63, doi:10.5194/hess-4-47-2000, 2000.

1520 Flury, M.: Experimental evidence of transport of pesticides through field soils - a review, J.  
1521 Environ. Qual., 25, 25-45, doi:10.2134/jeq1996.00472425002500010005x, 1996.

1522 Flury, M., Flühler, H., Leuenberger, J., and Jury, W. A.: Susceptibility of soils to preferential  
1523 flow of water: A field study, Water Resour. Res., 30, 1945-1954,  
1524 doi:10.1029/94WR00871, 1994.

1525 Flury, M., Leuenberger, J., Studer, B., and Flühler, H.: Transport of anions and herbicides in a  
1526 loamy and a sandy soil. , Water Resour. Res., 31, 823-835, doi:10.1029/94WR02852,  
1527 1995.

1528 Freeze, R. A. and Harlan, R. L.: Blueprint for a physically-based, digitally simulated  
1529 hydrologic response model, J. Hydrol., 9, 237-258, doi:10.1016/0022-1694(69)90020-1,  
1530 1969.

1531 Gao, H., Hrachowitz, M., Fenicia, F., Gharari, S., and Savenije, H. H. G.: Testing the realism  
1532 of a topography-driven model (flex-topo) in the nested catchments of the Upper Heihe,  
1533 China, Hydrol. Earth Syst. Sci., 18, 1895-1915, doi:10.5194/hess-18-1895-2014, 2014.

1534 Germann, P.: Preferential flow: Stokes approach to infiltration and drainage. Geographica  
1535 Bernensia, doi:10.4480/GB2018.G88, 2018

1536 Gharari, S., Hrachowitz, M., Fenicia, F., and Savenije, H. H. G.: Hydrological landscape  
1537 classification: Investigating the performance of hand based landscape classifications in a  
1538 central european meso-scale catchment, Hydrol. Earth Syst. Sci., 15, 3275-3291,  
1539 doi:10.5194/hess-15-3275-2011, 2011.

1540 Goldstein, H.: Classical Mechanics, Pearson Education Limited, Harlow, U.K., 2013.

1541 Goller, R., Wilcke, W., Fleischbein, K., Valarezo, C., and Zech, W., Dissolved nitrogen,  
1542 phosphorus, and sulfur forms in the ecosystem fluxes of a montane forest in Ecuador.  
1543 Biogeochemistry, 77, 57-89, doi:10.1007/s10533-005-1061-1, 2006.

1544 Gooseff, M. N., Wondzell, S. M., Haggerty, R., and Anderson, J.: Comparing transient  
1545 storage modeling and residence time distribution (RTD) analysis in geomorphically varied  
1546 reaches in the Lookout Creek basin, Oregon, USA, Adv. Water Resour., 26(9), 925-937,  
1547 doi:10.1016/S0309-1708(03)00105-2, 2003.

1548 Gouet-Kaplan, M. and Berkowitz, B.: Measurements of interactions between resident and  
1549 infiltrating water in a lattice micromodel, Vadose Zone J., 10, 624-633,  
1550 doi:10.2136/vzj2010.0103, 2011.

1551 Grayson, R. B., Moore, I. D. and McMahon, T. A.: Physically based hydrologic modeling: 2.  
1552 Is the concept realistic? Water Resour. Res., 28(10), 2659-2666, doi:10.1029/92WR01259,  
1553 1992.

1554 Gupta, H. V., Clark, M. P., Vrugt, J. A., Abramowitz, G. and Ye, M.: Towards a  
1555 comprehensive assessment of model structural adequacy, Water Resour. Res., 48(8), 1-16,  
1556 doi:10.1029/2011WR011044, 2012.

1557 Haggerty, R. and Gorelick S. M.: Multiple rate mass transfer for modeling diffusion and  
1558 surface reactions in media with pore-scale heterogeneity, Water Resour. Res., 31(10),  
1559 2383-2400, doi:10.1029/95WR10583, 1995.

1560 Haggerty, R., Wondzell, S. M., and Johnson, M. A.: Power-law residence time distribution in  
1561 the hyporheic zone of a 2nd-order mountain stream, Geophys. Res. Lett., 29(13), 18-1-18-  
1562 4, doi:10.1029/2002GL014743, 2002.



- 1563 Haken, H.: Synergetics: An introduction; nonequilibrium phase transitions and self-  
 1564 organization in physics, chemistry and biology, Springer Series in Synergetics, Springer  
 1565 Berlin, 355 pp., 1983.
- 1566 Hammel, K. and Roth, K.: Approximation of asymptotic dispersivity of conservative solute in  
 1567 unsaturated heterogeneous media with steady state flow, *Water Resour. Res.*, 34, 709-715,  
 1568 doi:10.1029/98WR00004, 1998.
- 1569 Harman, C. J.: Time-variable transit time distributions and transport: Theory and application  
 1570 to storage-dependent transport of chloride in a watershed, *Water Resour. Res.*, 51, 1-30,  
 1571 doi:10.1002/2014wr015707, 2015.
- 1572 He, Y., Bardossy, A., and Zehe, E.: A review of regionalisation for continuous streamflow  
 1573 simulation, *Hydrol. Earth Syst. Sci.*, 15, 3539-3553, doi:10.5194/hess-15-3539-2011,  
 1574 2011a.
- 1575 He, Y., Bardossy, A., and Zehe, E.: A catchment classification scheme using local variance  
 1576 reduction method, *J. Hydrol.*, 411, 140-154, doi:10.1016/j.jhydrol.2011.09.042, 2011b.
- 1577 Hergarten, S., Winkler, G., and Birk, S.: Transferring the concept of minimum energy  
 1578 dissipation from river networks to subsurface flow patterns, *Hydrol. Earth Syst. Sci.*, 18,  
 1579 4277-4288, doi:10.5194/hess-18-4277-2014, 2014.
- 1580 Hildebrandt, A., Kleidon, A., and Bechmann, M.: A thermodynamic formulation of root water  
 1581 uptake, *Hydrol. Earth Syst. Sci.*, 20, 3441-3454, doi:10.5194/hess-20-3441-2016, 2016.
- 1582 Hoffman, F., Ronen, D., Pearl, Z.: Evaluation of flow characteristics of a sand column using  
 1583 magnetic resonance imaging, *J. Contam. Hydrol.*, 22, 95-107, doi:10.1016/0169-  
 1584 7722(95)00079-8, 1996.
- 1585 Hopp, L., and McDonnell, J. J.: Connectivity at the hillslope scale: Identifying interactions  
 1586 between storm size, bedrock permeability, slope angle and soil depth, *J. Hydrol.*, 376(3-4),  
 1587 378-391, doi:10.1016/j.jhydrol.2009.07.047, 2009.
- 1588 Howard, A. D.: Optimal angles of stream junctions: geometric stability to capture and  
 1589 minimum power criteria, *Water Resour. Res.*, 7, 863-873, doi:10.1029/WR007i004p00863,  
 1590 1971.
- 1591 Howard, A. D.: Theoretical model of optimal drainage networks, *Water Resour. Res.*, 26,  
 1592 2107-2117, doi:10.1029/WR026i009p02107, 1990.
- 1593 Hrachowitz, M., and Clark, M. P.: HESS Opinions: The complementary merits of competing  
 1594 modelling philosophies in hydrology, *Hydrol. Earth Syst. Sci.*, 21, 3953-3973,  
 1595 doi:10.5194/hess-21-3953-2017, 2017.
- 1596 Hrachowitz, M., Benettin, P., van Breukelen, B. M., Fovet, O., Howden, N. J. K., Ruiz, L.,  
 1597 van der Velde, Y., and Wade, A. J.: Transit times – the link between hydrology and water  
 1598 quality at the catchment scale, *Wiley Interdisciplinary Reviews-Water*, 3, 629-657,  
 1599 doi:10.1002/wat2.1155, 2016.
- 1600 Hrachowitz, M., Fovet, O., Ruiz, L., and Savenije, H. H.: Transit time distributions, legacy  
 1601 contamination and variability in biogeochemical 1/f scaling: how are hydrological response  
 1602 dynamics linked to water quality at the catchment scale? *Hydrol. Proc.*, 29(25), 5241-5256,  
 1603 2015.
- 1604 Hrachowitz, M., Savenije, H., Boogard, T. A., Tetzlaff, D., and Soulsby, C.: What can flux  
 1605 tracking teach us about water age distribution patterns and their temporal dynamics?,  
 1606 *Hydrol. Earth Syst. Sciences*, 17, 533-564, doi:10.5194/hess-17-533-2013, 2013.

1607 Hrachowitz, M., Soulsby, C., Tetzlaff, D., Malcolm, I. A., and Schoups, G.: Gamma  
1608 distribution models for transit time estimation in catchments: Physical interpretation of  
1609 parameters and implications for time-variant transit time assessment, *Water Resour. Res.*,  
1610 46, W10536, doi:10.1029/2010WR009148, 2010.

1611 Hundecha, Y. and Bardossy, A.: Modeling of the effect of land use changes on the runoff  
1612 generation of a river basin through parameter regionalization of a watershed model, *J.*  
1613 *Hydrol.*, 292, 281-295, doi:10.1016/j.jhydrol.2004.01.002, 2004.

1614 Jackisch, C. and Zehe, E.: Ecohydrological particle model based on representative domains,  
1615 *Hydrol. Earth Syst. Sci.*, 22, 3639-3662, doi:10.5194/hess-22-3639-2018, 2018.

1616 Kapetas, L., Dror, I., and Berkowitz, B.: Evidence of preferential path formation and path  
1617 memory effect during successive infiltration and drainage cycles in uniform sand columns,  
1618 *J. Contam. Hydrol.*, 165, 1-10, doi:10.1016/j.jconhyd.2014.06.016., 2014.

1619 Kirchner, J. W.: A double paradox in catchment hydrology and geochemistry, *Hydrol. Proc.*,  
1620 17, 871-874, doi: 10.1002/hyp.5108, 2003.

1621 Kirchner, J. W.: Aggregation in environmental systems – Part 1: Seasonal tracer cycles  
1622 quantify young water fractions, but not mean transit times, in spatially heterogeneous  
1623 catchments, *Hydrol. Earth Syst. Sciences*, 279-297, doi:10.5194/hess-20-279-2016, 2016.

1624 Kirchner, J. W., Feng, X., and Neal, C.: Fractal stream chemistry and its implications for  
1625 contaminant transport in catchments, *Nature*, 403, 524-527, doi:10.1038/35000537, 2000.

1626 Klaus, J. and Zehe, E.: Modelling rapid flow response of a tile drained field site using a 2D-  
1627 physically based model: Assessment of “equifinal” model setups, *Hydrol. Proc.*, 24, 1595-  
1628 1609, doi:10.1002/hyp.7687, 2010.

1629 Klaus, J. and Zehe, E.: A novel explicit approach to model bromide and pesticide transport in  
1630 connected soil structures, *Hydrol. Earth Syst. Sci.*, 15, 2127-2144, doi:10.5194/hess-15-  
1631 2127-2011, 2011.

1632 Klaus, J., Zehe, E., Elsner, M., Kulls, C., and McDonnell, J. J.: Macropore flow of old water  
1633 revisited: Experimental insights from a tile-drained hillslope, *Hydrol. Earth Syst. Sci.*, 17,  
1634 103-118, doi:10.5194/hess-17-103-2013, 2013.

1635 Klaus, J., Zehe, E., Elsner, M., Palm, J., Schneider, D., Schroeder, B., Steinbeiss, S., van  
1636 Schaik, L., and West, S.: Controls of event-based pesticide leaching in natural soils: A  
1637 systematic study based on replicated field scale irrigation experiments, *J. Hydrol.*, 512,  
1638 528-539, doi:10.1016/j.jhydrol.2014.03.020, 2014.

1639 Klaus, J., Chun, K. P., McGuire, K. J., and McDonnell, J. J.: Temporal dynamics of  
1640 catchment transit times from stable isotope data, *Water Resour. Res.*, 51, 4208-4223,  
1641 doi:10.1002/2014wr016247, 2015.

1642 Kleidon, A.: How does the earth system generate and maintain thermodynamic disequilibrium  
1643 and what does it imply for the future of the planet?, *Philos. Trans. Royal Soc. A-Math.*  
1644 *Phys. Eng. Sci.*, 370, 1012-1040, doi:10.1098/rsta.2011.0316, 2012a.

1645 Kleidon, A., Zehe, E., and Lin, H.: Thermodynamic limits of the critical zone and their  
1646 relevance to hydrogeology, in: *Hydrogeology: Synergistic Integration of Soil Science*  
1647 *and Hydrology*, 5 Elsevier, Amsterdam, 854 pp., p. 243, 2012b.

1648 Kleidon, A., Zehe, E., Ehret, U., and Scherer, U.: Thermodynamics, maximum power, and the  
1649 dynamics of preferential river flow structures at the continental scale, *Hydrol. Earth Syst.*  
1650 *Sci.*, 17, 225-251, doi:10.5194/hess-17-225-2013, 2013.

1651 Koehler, B., Corre, M. D., Steger, K., Well, R., Zehe, E., Sueta, J. P., and Veldkamp, E.: An  
1652 in-depth look into a tropical lowland forest soil: Nitrogen-addition effects on the contents  
1653 of N<sub>2</sub>O, CO<sub>2</sub> and CH<sub>4</sub> and N<sub>2</sub>O isotopic signatures down to 2-m depth, *Biogeochemistry*,  
1654 111, 695-713, doi:10.1007/s10533-012-9711-6, 2012.

1655 Koehler, B., Zehe, E., Corre, M. D., and Veldkamp, E.: An inverse analysis reveals  
1656 limitations of the soil-CO<sub>2</sub> profile method to calculate CO<sub>2</sub> production and efflux for well-  
1657 structured soils, *Biogeosciences*, 7, 2311-2325, 10.5194/bg-7-2311-2010, 2010.

1658 Kondepudi, D., and Prigogine, I.: *Modern thermodynamics: From heat engines to dissipative*  
1659 *structures*, John Wiley Chichester, U.K., 1998.

1660 Lehmann, P., Hinz, C., McGrath, G., Tromp-van Meerveld, H. J., and McDonnell, J. J.:  
1661 Rainfall threshold for hillslope outflow: An emergent property of flow pathway  
1662 connectivity, *Hydrol. Earth Syst. Sci.*, 11, 1047-1063, doi:10.5194/hess-11-1047-2007,  
1663 2007.

1664 Levy, M. and Berkowitz, B.: Measurement and analysis of non-Fickian dispersion in  
1665 heterogeneous porous media, *J. Contam. Hydrol.*, 64(3-4), 203-226, doi:10.1016/S0169-  
1666 7722(02)00204-8, 2003.

1667 Lindstrom, G., Johansson, B., Persson, M., Gardelin, M., and Bergstrom, S.: Development  
1668 and test of the distributed HBV-96 hydrological model, *J. Hydrol.*, 201, 272-288,  
1669 doi:10.1016/S0022-1694(97)00041-3, 1997.

1670 Loritz, R., Hassler, S. K., Jackisch, C., Allroggen, N., van Schaik, L., Wienhöfer, J., and  
1671 Zehe, E.: Picturing and modeling catchments by representative hillslopes, *Hydrol. Earth*  
1672 *Syst. Sci.*, 21, 1225-1249, doi:10.5194/hess-21-1225-2017, 2017.

1673 Loritz, R., Gupta, H., Jackisch, C., Westhoff, M., Kleidon, A., Ehret, U., and Zehe, E.: On the  
1674 dynamic nature of hydrological similarity, *Hydrol. Earth Syst. Sci.*, 22, 3663-3684,  
1675 doi:10.5194/hess-22-3663-2018, 2018.

1676 Loritz, R., Kleidon, A., Jackisch, C., Westhoff, M., Ehret, U., Gupta, H., and Zehe, E.: A  
1677 topographic index explaining hydrological similarity by accounting for the joint controls of  
1678 runoff formation, *Hydrol. Earth Syst. Sci.*, 23, 3807-3821, doi:10.5194/hess-23-3807-2019,  
1679 2019.

1680 McDonnell, J. J.: The two water worlds hypothesis: Ecohydrological separation of water  
1681 between streams and trees?, *Wiley Interdisciplinary Reviews-Water*, 1, 323-329,  
1682 doi:10.1002/wat2.1027, 2014.

1683 McDonnell, J. J. and Beven, K.: Debates-the future of hydrological sciences: A (common)  
1684 path forward? A call to action aimed at understanding velocities, celerities and residence  
1685 time distributions of the headwater hydrograph, *Water Resour. Res.*, 50, 5342-5350,  
1686 doi:10.1002/2013wr015141, 2014.

1687 McGlynn, B. and Seibert, J.: Distributed assessment of contributing area and riparian  
1688 buffering along stream networks, *Water Resour. Res.*, 39, WR001521,  
1689 doi:10.1029/2002WR001521, 2003.

1690 McGlynn, B., McDonnell, J. J., Stewart, M., and Seibert, J.: On the relationships between  
1691 catchment scale and streamwater mean residence time, *Hydrol. Proc.*, 17, 175-181,  
1692 doi:10.1002/hyp.5085, 2002.

1693 McGrath, G. S., Hinz, C., and Sivapalan, M.: Modelling the impact of within-storm variability  
1694 of rainfall on the loading of solutes to preferential flow pathways, *Eur. J. Soil Sci.*, 59, 24-  
1695 33, doi:10.1111/j.1365-2389.2007.00987.x, 2008.

1696 McGrath, G. S., Hinz, C., Sivapalan, M., Dressel, J., Puetz, T., and Vereecken, H.: Identifying  
1697 a rainfall event threshold triggering herbicide leaching by preferential flow, *Water Resour.*  
1698 *Res.*, 46, W02513, doi:10.1029/2008wr007506, 2010.

1699 Mertens, J., Madsen, H., Feyen, L., Jacques, D., and Feyen, J.: Including prior information in  
1700 the estimation of effective soil parameters in unsaturated zone modelling, *J. Hydrol.*, 294,  
1701 251-269, 2004.

1702 Milne, G.: Normal erosion as a factor in soil profile development. *Nature*, 138, 548-549,  
1703 doi:10.1038/138548c0, 1936.

1704 Nash, J. E.: The form of the instantaneous unit hydrograph, IASH publication no. 45, 3-4,  
1705 114-121, 1957.

1706 Niemi, A. J.: Residence time distribution of variable flow processes, *Int. J. Appl. Radiat. Isot.*,  
1707 28, 855-860, doi:10.1016/0020-708X(77)90026-6, 1977.

1708 Nissan, A. and Berkowitz, B.: Anomalous transport dependence on Péclet number, porous  
1709 medium heterogeneity, and a temporally varying velocity field, *Phys. Rev. E*, 99, 033108,  
1710 doi:10.1103/PhysRevE.99.033108, 2019.

1711 Nissan, A., Dror, I., and Berkowitz, B.: Time-dependent velocity-field controls on anomalous  
1712 chemical transport in porous media, *Water Resour. Res.*, 53, 3760-3769,  
1713 doi:10.1002/2016WR020143, 2017.

1714 Oswald, S., Kinzelbach, W., Greiner, A., and Brix, G.: Observation of flow and transport  
1715 processes in artificial porous media via magnetic resonance imaging in three dimensions,  
1716 *Geoderma*, 80, 417-429, doi:10.1016/S0016-7061(97)00064-5, 1997.

1717 Paik, K. and Kumar, P.: Optimality approaches to describe characteristic fluvial patterns on  
1718 landscapes, *Philos. Trans. R. Soc. B-Biol. Sci.*, 365, 1387-1395,  
1719 doi:10.1098/rstb.2009.0303, 2010.

1720 Paltridge, G. W.: Climate and thermodynamic systems of maximum dissipation, *Nature*, 279,  
1721 630-631, doi:10.1038/279630a0, 1979.

1722 Refsgaard, J. C. and Storm, B.: MikeShe, in: *Computer models of watershed hydrology*,  
1723 edited by: Singh, V. P., Water Resources Publications, Highland Ranch, Colorado, USA,  
1724 809-846, 1995.

1725 Reinhardt, L., and Ellis, M. A.: The emergence of topographic steady state in a perpetually  
1726 dynamic self organised critical landscape, *Water Resour. Res.*, 51, 4986-5003,  
1727 doi:10.1002/2014WR016223, 2015.

1728 Rinaldo, A., Maritan, A., Colaiori, F., Flammini, A., and Rigon, R.: Thermodynamics of  
1729 fractal networks, *Phys. Rev. Lett.*, 76, 3364-3367, doi:10.1103/PhysRevLett.76.3364,  
1730 1996.

1731 Rinaldo, A., Benettin, P., Harman, C. J., Hrachowitz, M., McGuire, K. J., van der Velde, Y.,  
1732 Bertuzzo, E., and Botter, G.: Storage selection functions: A coherent framework for  
1733 quantifying how catchments store and release water and solutes, *Water Resour. Res.*, 51,  
1734 4840-4847, doi:10.1002/2015wr017273, 2015.

1735 Rodriguez, N. B., and Klaus, J.: Catchment travel times from composite storage selection  
1736 functions representing the superposition of streamflow generation processes, *Water*  
1737 *Resour. Res.*, 55, 9292-9314, doi:10.1029/2019wr024973, 2019.

1738 Rodriguez, N. B., McGuire, K. J., and Klaus, J.: Time-varying storage-water age relationships  
1739 in a catchment with a mediterranean climate, *Water Resour. Res.*, 54, 3988-4008,  
1740 doi:10.1029/2017wr021964, 2018.

1741 Rodriguez, N. B., Pfister, L., Zehe, E., and Klaus, J.: Testing the truncation of travel times  
1742 with StorAge Selection functions using deuterium and tritium as tracers. *Hydrology and*  
1743 *Earth System Sciences*, submitted, 2019.

1744 Rodriguez-Iturbe, I. and Rinaldo, A.: *Fractal river basins: Chance and self-organization*,  
1745 Cambridge Univ. Press, Cambridge U. K., 2001.

1746 Rodriguez-Iturbe, I., D'Odorico, P., Porporato, A., and Ridolfi, L.: On the spatial and  
1747 temporal links between vegetation, climate, and soil moisture, *Water Resour. Res.*, 35,  
1748 3709-3722, doi:10.1029/1999wr900255, 1999.

1749 Roth, K. and Hammel, K.: Transport of conservative chemical through an unsaturated two-  
1750 dimensional Miller-similar medium with steady state flow, *Water Resour. Res.*, 32, 1653-  
1751 1663, doi: 10.1029/96WR00756, 1996.

1752 Samaniego, L. and Bardossy, A.: Simulation of the impacts of land use/cover and climatic  
1753 changes on the runoff characteristics at the mesoscale, *Ecol. Model.*, 196, 45-61,  
1754 doi:10.1016/j.ecolmodel.2006.01.005, 2006.

1755 Sander, T. and Gerke, H. H.: Modelling field-data of preferential flow in paddy soil induced  
1756 by earthworm burrows, *J. Contam Hydrol.*, 104, 126-136,  
1757 doi:10.1016/j.jconhyd.2008.11.003, 2009.

1758 Savenije, H. H. G.: HESS Opinions "Topography driven conceptual modelling (flex-topo)",  
1759 *Hydrol. Earth Syst. Sci.*, 14, 2681-2692, doi:10.5194/hess-14-2681-2010, 2010.

1760 Savenije, H. H. G. and Hrachowitz, M.: HESS Opinions "Catchments as meta-organisms - a  
1761 new blueprint for hydrological modelling", *Hydrol. Earth Syst. Sci.*, 21, 1107-1116,  
1762 doi:10.5194/hess-21-1107-2017, 2017.

1763 Scheidegger, A. E.: An evaluation of the accuracy of the diffusivity equation for describing  
1764 miscible displacement in porous media, *Proc. Theory Fluid Flow Porous Media 2<sup>nd</sup> Conf.*,  
1765 101-116, 1959.

1766 Scher, H. and Montroll, E. W.: Anomalous transit time dispersion in amorphous solids, *Phys.*  
1767 *Rev. B*, 12, 2455-2477, doi:10.1103/PhysRevB.12.2455, 1975.

1768 Scher, H., Margolin, G., Metzler, R., Klafter, J., and Berkowitz, B.: The dynamical foundation  
1769 of fractal stream chemistry: The origin of extremely long retention times, *Geophys. Res.*  
1770 *Let.*, 29(5), doi:10.1029/2001GL014123, 2002.

1771 Shannon, C. E.: A mathematical theory of communication, *Bell Syst. Tech.*, J. 27, 379-423.  
1772 doi:10.1145/584091.584093, 1948.

1773 Sherman, L. K.: Streamflow from rainfall by the unit hydrograph method, *Eng. News Record*,  
1774 180, 501-505, 1932.

1775 Simmons, C. S.: A stochastic-convective transport representation of dispersion in one  
1776 dimensional porous media systems, *Water Resour. Res.*, 18, 1193-1214,  
1777 doi:10.1029/WR018i004p01193, 1982.

1778 Šimunek, J., Jarvis, N. J., van Genuchten, M. T., and Gardenas, A.: Review and comparison  
1779 of models for describing non-equilibrium and preferential flow and transport in the vadose  
1780 zone, *J. Hydrol.*, 272, 14-35, doi:10.1016/S0022-1694(02)00252-4, 2003.

1781 Singh, S. K., McMillan, H., Bardossy, A., and Fateh, C.: Nonparametric catchment clustering  
1782 using the data depth function, *Hydrol. Sci. J.-J. Sci. Hydrol.*, 61, 2649-2667,  
1783 doi:10.1080/02626667.2016.1168927, 2016.

1784 Sivapalan, M.: From engineering hydrology to earth system science: Milestones in the  
1785 transformation of hydrologic science, *Hydrol. Earth Syst. Sci.*, 22, 1665-1693, doi:  
1786 doi:10.5194/hess-22-1665-2018, 2018.

1787 Sklash, M. G., and Farvolden, R. N.: The role of groundwater in storm runoff, *J. Hydrol.*, 43,  
1788 45-65, doi: 10.1016/0022-1694(79)90164-1, 1979.

1789 Sklash, M. G., Beven, K. J., Gilman, K., and Darling, W. G.: Isotope studies of pipeflow at  
1790 plynlimon, wales, UK, *Hydrol. Proc.*, 10, 921-944, doi:10.1002/(SICI)1099-  
1791 1085(199607)10:7<921::AID-HYP347>3.0.CO;2-B, 1996.

1792 Sposito, G., Jury, W. A., and Gupta, V. K.: Fundamental problems in the stochastic  
1793 convection-dispersion model of solute transport in aquifers and field soils, *Water Resour.*  
1794 *Res.*, 22(1), 77-88, 1986.

1795 Sprenger, M., Tetzlaff, D., Buttle, J., Laudon, H., Leistert, H., Mitchell, C. P. J., Snelgrove, J.,  
1796 Weiler, M., and Soulsby, C.: Measuring and modeling stable isotopes of mobile and bulk  
1797 soil water, *Vadose Zone J.*, 17, 1-18, doi:10.2136/vzj2017.08.0149, 2018.

1798 Sternagel, A., Loritz, R., Wilcke, W., and Zehe, E.: Simulating preferential soil water flow  
1799 and tracer transport using the Lagrangian Soil Water and Solute Transport Model, *Hydrol.*  
1800 *Earth Syst. Sci. Discuss.*, doi:10.5194/hess-2019-132, accepted 2019.

1801 Tromp-van Meerveld, H. J., and McDonnell, J. J.: Threshold relations in subsurface  
1802 stormflow: 2. The fill and spill hypothesis, *Water Resour. Res.*, 42, W02411,  
1803 doi:10.1029/2004wr003800, 2006.

1804 Turton, D. J., Barnes, D. R., and de Jesus Navar, J.: Old and new water in subsurface flow  
1805 from a forest soil block, *J. Environ. Qual.*, 24, 139-146,  
1806 doi:10.2134/jeq1995.00472425002400010020x, 1995.

1807 van der Velde, Y., Torfs, P. J. J. F., van der Zee, S. E. A. T. M., and Uijlenhoet, R.:  
1808 Quantifying catchment scale mixing and its effect on time varying travel time distributions.  
1809 *Water Resour. Res.*, 48, W06536, doi:10.1029/2011WR011310, 2012.

1810 van Schaik, L., Palm, J., Klaus, J., Zehe, E., and Schröder, B.: Linking spatial earthworm  
1811 distribution to macropore numbers and hydrological effectiveness, *Ecohydrology*, 7, 401-  
1812 408, doi:10.1002/eco.1358, 2014.

1813 Vogel, H. J. and Roth, K.: Quantitative morphology and network representation of soil pore  
1814 structure, *Adv. Water Resour.*, 24, 233-242, doi:10.1016/S0309-1708(00)00055-5, 2001.

1815 Vogel, H. J., Cousin, I., Ippisch, O., and Bastian, P.: The dominant role of structure for solute  
1816 transport in soil: Experimental evidence and modelling of structure and transport in a field  
1817 experiment, *Hydrol. Earth Syst. Sci.*, 10, 495-506, doi:10.5194/hess10-495-2006, 2006.

1818 Vrugt, J. A. and Ter Braak, C. J. F.: Dream((d)): An adaptive markov chain monte carlo  
1819 simulation algorithm to solve discrete, noncontinuous, and combinatorial posterior  
1820 parameter estimation problems, *Hydrol. Earth Syst. Sci.*, 15, 3701-3713, doi:10.5194/hess-  
1821 15-3701-2011, 2011.

1822 Wagener, T., and Wheater, H. S.: Parameter estimation and regionalization for continuous  
1823 rainfall-runoff models including uncertainty, *J. Hydrol.*, 320, 132-154, 2006.

1824 Weiler, M., McGlynn, B. L., McGuire, K. J., and McDonnell, J. J.: How does rainfall become  
1825 runoff? A combined tracer and runoff transfer function approach, *Water Resour. Res.*, 39,  
1826 1315, doi:10.1029/2003wr002331, 2003.

1827 Weinberg, G. M. (1975). *An Introduction to General Systems Thinking*. New York: John  
1828 Wiley & Sons, N.Y., p. 279.

1829 Westhoff, M. C. and Zehe, E.: Maximum entropy production: Can it be used to constrain  
1830 conceptual hydrological models?, *Hydrol. Earth Syst. Sci.*, 17, 3141-3157,  
1831 doi:10.5194/hess-17-3141-2013, 2013.

1832 Westhoff, M., Kleidon, A., Schymanski, S., Dewals, B., Nijse, F., Renner, M., Dijkstra, H.,  
1833 Ozawa, H., Savenije, H., Dolman, H., Meesters, A., and Zehe, E.: ESD Reviews:  
1834 Thermodynamic optimality in Earth sciences. The missing constraints in modeling Earth  
1835 system dynamics? *Earth Syst. Dynam. Discuss.*, doi:10.5194/esd-2019-6, in review, 2019.

1836 Westhoff, M., Zehe, E., Archambeau, P., and Dewals, B.: Does the Budyko curve reflect a  
1837 maximum-power state of hydrological systems? A backward analysis, *Hydrol. Earth Syst.*  
1838 *Sci.*, 20, 479-486, doi:10.5194/hess-20-479-2016, 2016.

1839 Wienhoefer, J. and Zehe, E.: Predicting subsurface stormflow response of a forested hillslope  
1840 - the role of connected flow paths, *Hydrol. Earth Syst. Sci.*, 18, 121-138, doi:10.5194/hess-  
1841 18-121-2014, 2014.

1842 Wienhofer, J., Germer, K., Lindenmaier, F., Farber, A., and Zehe, E.: Applied tracers for the  
1843 observation of subsurface stormflow at the hillslope scale, *Hydrol. Earth Syst. Sci.*, 13,  
1844 1145-1161, doi:10.5194/hess-13-1145-2009, 2009.

1845 Wilcke, W., Yasin, S., Valarezo, C., and Zech, W.: Change in water quality during the  
1846 passage through a tropical montane rain forest in Ecuador. *Biogeochemistry* 55, 45-72,  
1847 doi:10.1023/A:1010631407270, 2001.

1848 Worthington, S. R. H. and Ford D. C.: Self-organised permeability in carbonate aquifers,  
1849 *Groundwater*, 47(3), 326-336, doi:10.1111/j.1745-6584.2009.00551.x, 2009.

1850 Wrede, S., Fenicia, F., Martinez-Carreras, N., Juilleret, J., Hissler, C., Krein, A., Savenije, H.  
1851 H. G., Uhlenbrook, S., Kavetski, D., and Pfister, L.: Towards more systematic perceptual  
1852 model development: A case study using 3 Luxembourgish catchments, *Hydrol. Proc.*, 29,  
1853 2731-2750, doi:10.1002/hyp.10393, 2015.

1854 Zehe, E. and Jackisch, C.: A Lagrangian model for soil water dynamics during rainfall-driven  
1855 conditions, *Hydrol. Earth Syst. Sci.*, 20, 3511-3526, doi:10.5194/hess-20-3511-2016, 2016.

1856 Zehe, E., Blume, T., and Blöschl, G.: The principle of 'maximum energy dissipation': A novel  
1857 thermodynamic perspective on rapid water flow in connected soil structures, *Philos. Trans.*  
1858 *R. Soc. B-Biol. Sci.*, 365, 1377-1386, doi:10.1098/rstb.2009.0308, 2010.

1859 Zehe, E., Ehret, U., Blume, T., Kleidon, A., Scherer, U., and Westhoff, M.: A thermodynamic  
1860 approach to link self-organization, preferential flow and rainfall-runoff behaviour, *Hydrol.*  
1861 *Earth Syst. Sci.*, 17, 4297-4322, doi:10.5194/hess-17-4297-2013, 2013.

1862 Zehe, E., Ehret, U., Pfister, L., Blume, T., Schroder, B., Westhoff, M., Jackisch, C.,  
1863 Schymanski, S. J., Weiler, M., Schulz, K., Allroggen, N., Tronicke, J., van Schaik, L.,  
1864 Dietrich, P., Scherer, U., Eccard, J., Wulfmeyer, V., and Kleidon, A.: Hess opinions: From  
1865 response units to functional units: A thermodynamic reinterpretation of the hru concept to



1866 link spatial organization and functioning of intermediate scale catchments, *Hydrol. Earth*  
1867 *Syst. Sci.*, 18, 4635-4655, doi:10.5194/hess-18-4635-2014, 2014.  
1868 Zehe, E., Loritz, R., Jackisch, C., Westhoff, M., Kleidon, A., Blume, T., Hassler, S. K., and  
1869 Savenije, H. H.: Energy states of soil water – a thermodynamic perspective on soil water  
1870 dynamics and storage-controlled streamflow generation in different landscapes, *Hydrol.*  
1871 *Earth Syst. Sci.*, 23, 971-987, doi:10.5194/hess-23-971-2019, 2019.  
1872 Zhang, Y., Benson, D. A., and Reeves, D. M.: Time and space nonlocalities underlying  
1873 fractional-derivative models: Distinction and review of field applications, *Adv. Water*  
1874 *Resour.*, 32, 561-581, doi:10.1016/j.advwatres.2009.01.008, 2009.